

# Some bivariate distributions on a discrete torus with application to wind direction datasets

Brajesh Kumar Dhakad<sup>1</sup>, Jayant Jha<sup>2</sup>, Debepsita Mukherjee<sup>3</sup>

<sup>1</sup>Department of Mathematics, Indian Institute of Technology Madras,  
IIT P.O., Sardar Patel Road, Chennai, 600036, Tamil Nadu, India.

<sup>2</sup>Statistical Sciences Division, Indian Statistical Institute, Kolkata, 203  
B. T. Road, Kolkata, 700108, West Bengal, India.

<sup>3</sup>Department of Statistics and Data Sciences, University of Texas at  
Austin, 105 East 24th St. Stop D9800, Austin, 78712, Texas, USA.

Contributing authors: [brajeshdhakad85047@gmail.com](mailto:brajeshdhakad85047@gmail.com);  
[jayantjha@gmail.com](mailto:jayantjha@gmail.com); [debepsitamukherjee@gmail.com](mailto:debepsitamukherjee@gmail.com);

## Abstract

Many datasets are observed on a finite set of equally spaced directions instead of the exact angles, such as the wind direction data. However, in the statistical literature, bivariate models are only available for continuous circular random variables. This article presents two bivariate circular distributions, namely bivariate wrapped geometric (BWG) and bivariate generalized wrapped geometric (BGWG), for analyzing bivariate discrete circular data. We consider wrapped geometric distributions and a trigonometric function to construct the models. The models are analytically tractable due to the exact closed-form expressions for the trigonometric moments. We thoroughly discuss the distributional properties of the models, including the interpretation of parameters and dependence structure. The estimation methodology based on maximizing the likelihood functions is illustrated for simulated datasets. Finally, the proposed distributions are utilized to analyze pairwise wind direction measurements obtained at different stations in India, and the interpretations for the fitted models are briefly discussed.

**Keywords:** Circular correlation, Circular data, Discrete bivariate circular distribution, Discrete torus, Trigonometric moments

# 1 Introduction

Directional statistics deals with data measured as angles, axes, or rotations. Its applications have grown rapidly in the fields of biology, neuroscience, environmental science, meteorology, and computer vision. Extensive reviews of these fields and applications are provided by [17, 4, 8, 19, 21]. In some areas, a particularly important case is the study of bivariate circular data, which arises when two directions are observed simultaneously. For example, this involves analyzing pairs of wind directions, recorded at two different locations, altitudes, or time points.

Although wind direction is inherently continuous, in practice, it is routinely observed on a finite set of equally spaced directions. Data from meteorological stations, wave buoys, and animal-orientation sensors are typically reported in 4, 8, 16, or even 36 categories. These measurements form ordinal circular data, where the categories  $x_1, x_2, \dots, x_n$  wrap around the circle (the neighbours of  $x_1$  are  $x_2$  and  $x_n$ ), whereas in ordinal linear data,  $x_1$  is the farthest from  $x_n$ . This structure necessitates statistical models for ordinal circular variables.

Existing models for bivariate circular data are defined for continuous variables. For instance, the distributions over the torus are examined in [18], the bivariate von Mises distribution and the bivariate wrapped Cauchy distribution are discussed in [20, 13] respectively. Copula-based approaches are considered by [11, 16], and a multimodal bivariate circular distribution is proposed in [5]. Some circular–circular regression models are discussed in [14], [10], and [15]. However, adapting them to bivariate ordinal circular data requires double integration over rectangular regions, which rarely yields a closed form. This necessitates the use of numerical integration methods, which impose computational burden and inevitably introduce approximation errors.

In the context of ordinal circular data, literature has focused on univariate models, including the wrapped Poisson distribution [1], the wrapped geometric distribution [7], and the wrapped symmetric geometric (WSG) distribution [9], but no analytically tractable bivariate model is available for the discrete torus. Therefore, a discrete toroidal distribution is needed.

A direct application of discrete toroidal distributions can be seen in Indian climatology. As noted by [23] (Chapter 2), India’s unique physiography, which is characterized by the Himalayas in the north, the tapering peninsula to the south, and hill ranges across the northwest, northeast, and west coast, plays a decisive role in its climate. During winter (Dec-Feb), a high-pressure system north of the Himalayas drives dry continental winds southward, where they interact with local topography and trade winds. These winds demonstrate interconnected dynamics across different parts of the country (see [2, 22] for more information). Understanding the relationship between wind directions at stations separated by hundreds of kilometers is essential for wind energy planning, air pollution dispersion, and structural engineering. Typically, meteorological records in India report wind direction in 16 sectors ( $22.5^\circ$  intervals), making discrete bivariate circular models directly applicable.

This paper proposes analytically tractable bivariate distributions for data on a discrete torus, constructed by combining the WSG distributions with a trigonometric linking function. Closed form expressions are derived for the joint pmf, marginals,

conditionals, modes, and a circular–circular correlation measure. Proposed distributions are applied to pairwise wind direction data from three Indian stations (Gwalior, Chennai, and Mangaluru).

The performance of the proposed models is evaluated through a comparison with discretized versions of prominent continuous distributions: the bivariate wrapped Cauchy [13] and the von Mises Sine and Cosine distributions [20].

This article is organized as follows: in Section 2, the proposed bivariate ordinal circular distribution is introduced, and in Section 3, its relevant properties are discussed. Section 4 generalizes the bivariate ordinal circular distribution. Section 5 extends the discussion on model parameters. Section 6 studies the proposed models using simulated data. Section 7 shows the application of the models for analyzing three bivariate wind direction datasets. Section 8 concludes.

## 2 Bivariate model for ordinal circular data

We briefly discuss the WSG distribution in Subsection 2.1 for univariate ordinal circular data. Then, in Subsection 2.2, we construct a bivariate distribution based on WSG and a cosine function.

### 2.1 Wrapped symmetric geometric distribution

Let  $\mathbb{Z}_+$  denotes the set of positive integers,  $\mathbf{Z}_m$  the cyclic group of integers of order  $m$ , and  $\mathbf{D}_m$  the domain consisting of the vertices of a regular polygon, i.e.,

$$\mathbf{Z}_m = \{0, 1, \dots, m-1\}, \quad \text{and} \quad \mathbf{D}_m = \left\{ \frac{2\pi r}{m}, r \in \mathbf{Z}_m \right\}, \quad \text{where } m \in \mathbb{Z}_+. \quad (1)$$

The probability mass function (pmf) of a discrete random variable is denoted as  $P(\cdot)$ . The pmf of the discrete random variable  $X$ , defined on  $\mathbf{D}_m$ , is given as

$$P\left(\frac{2\pi k}{m}\right) = \left( \frac{1-q}{(1-q^m)(1+q)} \right) (q^\zeta + q^{m-\zeta}), \quad k \in \mathbf{Z}_m, \quad (2)$$

where  $q \in (0, 1)$ ,  $\zeta = (k - \alpha) \bmod m$ , and  $\alpha \in \mathbf{Z}_m$ . The distribution given in (2) is called a wrapped symmetric geometric distribution for ordinal circular data and is explored in [9]. It is a unimodal symmetric distribution whose modal direction is  $\frac{2\pi\alpha}{m}$ . The WSG distribution is undefined for  $q \in \{0, 1\}$ ; these cases are examined by evaluating the limit of the pmf (2). When  $q = 0$ , it degenerates at  $\frac{2\pi\alpha}{m}$ , whereas for  $q = 1$ , it becomes uniform.

The study of bivariate wind directions motivates the need for a generalization of the WSG distribution. In Subsection 2.2, we present a bivariate distribution on the discrete torus whose sample space is  $\mathbf{D}_{m_1} \times \mathbf{D}_{m_2} = \left\{ \frac{2\pi k}{m_1}, k \in \mathbf{Z}_{m_1} \right\} \times \left\{ \frac{2\pi l}{m_2}, l \in \mathbf{Z}_{m_2} \right\}$ , which represents  $m_1 \times m_2$  grid points on the torus.

## 2.2 Bivariate wrapped geometric distribution

The random variable  $(X_1, X_2)$  is the bivariate circular random variable defined on  $\mathbf{D}_{\mathbf{m}_1} \times \mathbf{D}_{\mathbf{m}_2}$ , and its pmf is denoted by  $P(\cdot, \cdot)$ . It can be written as

$$P\left(\frac{2\pi k}{m_1}, \frac{2\pi l}{m_2}\right) = P\left(X_1 = \frac{2\pi k}{m_1}, X_2 = \frac{2\pi l}{m_2}\right), \quad k \in \mathbf{Z}_{\mathbf{m}_1}, l \in \mathbf{Z}_{\mathbf{m}_2}.$$

The proposed joint distribution of  $(X_1, X_2)$  is given by:

$$P\left(\frac{2\pi k}{m_1}, \frac{2\pi l}{m_2}\right) \propto (q^{\zeta_1} + q^{m_1 - \zeta_1})(s^{\zeta_2} + s^{m_2 - \zeta_2}) \left(1 + \rho \cos\left(\frac{2\pi\zeta_1}{m_1} - \delta \frac{2\pi\zeta_2}{m_2}\right)\right), \quad (3)$$

where  $\zeta_1 = (k - \alpha) \bmod m_1$  and  $\zeta_2 = (l - \beta) \bmod m_2$ . The parameters are  $\alpha \in \mathbf{Z}_{m_1}$ ,  $\beta \in \mathbf{Z}_{m_2}$ ,  $\rho \in [-1, 1]$ ,  $\delta \in \{-1, 1\}$  and  $q, s \in (0, 1)$ .

The proposed distribution has a copula interpretation similar to that of the circula described in [11], where the circula employs the discrete version of cardioid density defined by

$$g\left(\frac{2\pi k}{m}\right) = \frac{1}{m} \left(1 + \rho \cos\left(\frac{2\pi\zeta}{m}\right)\right).$$

Next, we derive a few theorems and corollaries related to the proposed distribution, and all proofs are given in the Appendix.

**Theorem 1** *The closed form expression for the proposed joint pmf of  $(X_1, X_2)$  is given by*

$$P\left(\frac{2\pi k}{m_1}, \frac{2\pi l}{m_2}\right) = C_1 (q^{\zeta_1} + q^{m_1 - \zeta_1})(s^{\zeta_2} + s^{m_2 - \zeta_2}) \left(1 + \rho \cos\left(\frac{2\pi\zeta_1}{m_1} - \delta \frac{2\pi\zeta_2}{m_2}\right)\right), \quad (4)$$

where,  $C_1 = \frac{(1-q)(1-s)}{(1-q^{m_1})(1-s^{m_2})(1+q)(1+s)} \left( \frac{(q^2 - 2q \cos \frac{2\pi}{m_1} + 1)(s^2 - 2s \cos \frac{2\pi}{m_2} + 1)}{(q^2 - 2q \cos \frac{2\pi}{m_1} + 1)(s^2 - 2s \cos \frac{2\pi}{m_2} + 1) + \rho(1-q)^2(1-s)^2} \right)$ .

The distribution given in (4), referred to as ‘‘bivariate wrapped geometric’’ (BWG) distribution, is a discrete bivariate circular distribution symmetric around  $\left(\frac{2\pi\alpha}{m_1}, \frac{2\pi\beta}{m_2}\right)$ .

Since the BWG distribution is not defined when parameters  $q$  or  $s$  take values in  $\{0, 1\}$ , the distributions for these cases are derived by evaluating the limits of the pmf (4). The results are summarized in Table 1.

## 3 Properties of the model

In this section, we discuss some properties of the BWG distribution, including the role of parameters in the dependence structure of  $(X_1, X_2)$ , the dominant mode, and the marginal and conditional distributions.

**Corollary 1** *In the BWG distribution, the random variables  $X_1$  and  $X_2$  are independent when  $\rho = 0$ .*

Corollary 1 highlights the importance of examining the role of  $\rho$  in the dependence structure of  $(X_1, X_2)$ . To graphically illustrate the effect of  $\rho$ , we fix  $m_1 = m_2 =$

5,  $q = s = 0.5$ ,  $\alpha = \beta = 2$ , and  $\delta = 1$ . Figure 1 presents the probability mass plot of the BWG distribution for various values of  $\rho$ .

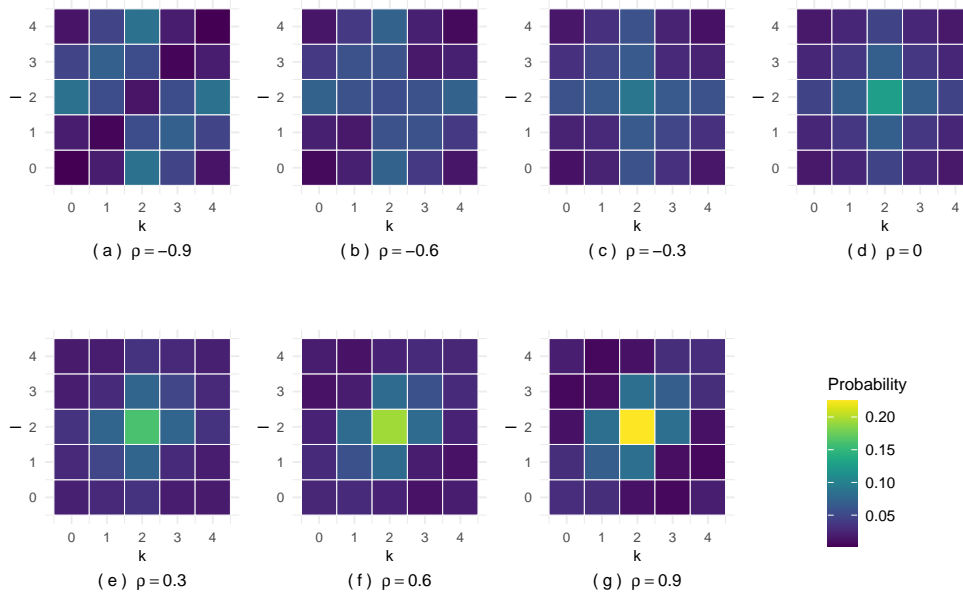


**Fig. 1:** Probability mass plot of BWG distribution for various values of  $\rho$

In Figure 1, the cell  $(k, l)$  represents the location  $\left(\frac{2\pi k}{m_1}, \frac{2\pi l}{m_2}\right)$ . Subfigures (a) and (b) illustrate that the location of the dominant mode (i.e., the point of highest probability) is not unique. Specifically,  $(0, 4\pi/5)$ ,  $(8\pi/5, 4\pi/5)$ ,  $(4\pi/5, 0)$ , and  $(4\pi/5, 8\pi/5)$  are the locations of the highest probabilities. Notably, the cells  $(0, 2)$  and  $(4, 2)$  are neighbors, and similarly,  $(2, 0)$  and  $(2, 4)$ . In contrast, subfigures (c) to (g) demonstrate that the location of the dominant mode is unique at  $\left(\frac{2\pi\alpha}{m_1}, \frac{2\pi\beta}{m_2}\right)$ . We observe that for  $\rho \geq 0$ , the location of the dominant mode remains unique at this location; however, when  $\rho < 0$ , the location of the dominant mode may not be unique.

**Theorem 2** For  $\rho \geq 0$ , the BWG distribution has a dominant mode at  $\left(\frac{2\pi\alpha}{m_1}, \frac{2\pi\beta}{m_2}\right)$ . Further, excluding the case  $q = s = 1$ , this mode is unique.

This result indicates that when  $\rho$  is positive, the BWG distribution attains its highest probability at  $\left(\frac{2\pi\alpha}{m_1}, \frac{2\pi\beta}{m_2}\right)$ . However, in the limiting case where  $q = s = 1$ , the behavior depends on  $\rho$ . For  $\rho > 0$ , the distribution achieves its maximum over the set  $\left\{\left(\frac{2\pi k}{m_1}, \frac{2\pi l}{m_2}\right) : \cos\left(\frac{2\pi\zeta_1}{m_1} - \delta\frac{2\pi\zeta_2}{m_2}\right) = 1\right\}$ , whereas if  $\rho = 0$ , it becomes the uniform distribution. These limiting cases are summarized in Table 1.

**Table 1:** Limits of pmf (4) on boundaries of parameter space

$(q, s)$	pmf $P(\cdot, \cdot)$
$\{0\} \times (0, 1)$	$\begin{cases} C_2(s^{\zeta_2} + s^{m_2 - \zeta_2})(1 + \rho \cos \frac{2\pi\zeta_2}{m_2}) & \text{if } k = \alpha, l \in \mathbf{Z}_{m_2} \\ 0 & \text{else,} \end{cases}$ where $C_2 = \left( \frac{1}{(1-s^{m_2})(1+s)} \right) \left( \frac{(1-s)(s^2 - 2s \cos \frac{2\pi}{m_2} + 1)}{s^2 - 2s \cos \frac{2\pi}{m_2} + 1 + \rho(1-s)^2} \right)$
$(0, 1) \times \{0\}$	$\begin{cases} C_3(q^{\zeta_1} + q^{m_1 - \zeta_1})(1 + \rho \cos \frac{2\pi\zeta_1}{m_1}) & \text{if } k \in \mathbf{Z}_{m_1}, l = \beta \\ 0 & \text{else,} \end{cases}$ where $C_3 = \left( \frac{1}{(1-q^{m_1})(1+q)} \right) \left( \frac{(1-q)(q^2 - 2q \cos \frac{2\pi}{m_1} + 1)}{q^2 - 2q \cos \frac{2\pi}{m_1} + 1 + \rho(1-q)^2} \right)$
$\{0\} \times \{0\}$	$\begin{cases} 1 & \text{if } k = \alpha, l = \beta \\ 0 & \text{else} \end{cases}$
$\{1\} \times (0, 1)$	$\frac{1}{m_1} \left( \frac{(1-s)(s^{\zeta_2} + s^{m_2 - \zeta_2})}{(1-s^{m_2})(1+s)} \right) \left( 1 + \rho \cos \left( \frac{2\pi\zeta_1}{m_1} - \delta \frac{2\pi\zeta_2}{m_2} \right) \right)$
$(0, 1) \times \{1\}$	$\frac{1}{m_2} \left( \frac{(1-q)(q^{\zeta_1} + q^{m_1 - \zeta_1})}{(1-q^{m_1})(1+q)} \right) \left( 1 + \rho \cos \left( \frac{2\pi\zeta_1}{m_1} - \delta \frac{2\pi\zeta_2}{m_2} \right) \right)$
$\{1\} \times \{1\}$	$\frac{1}{m_1 \times m_2} \left( 1 + \rho \cos \left( \frac{2\pi\zeta_1}{m_1} - \delta \frac{2\pi\zeta_2}{m_2} \right) \right)$
$\{1\} \times \{0\}$	$\begin{cases} \frac{1}{m_1} (1 + \rho \cos \frac{2\pi\zeta_1}{m_1}) & \text{if } k \in \mathbf{Z}_{m_1}, l = \beta \\ 0 & \text{else} \end{cases}$
$\{0\} \times \{1\}$	$\begin{cases} \frac{1}{m_2} (1 + \rho \cos \frac{2\pi\zeta_2}{m_2}) & \text{if } k = \alpha, l \in \mathbf{Z}_{m_2} \\ 0 & \text{else} \end{cases}$

### 3.1 Marginal wrapped symmetric geometric distribution

The marginal distribution of  $X_1$  is given as

$$P\left(\frac{2\pi k}{m_1}\right) = \sum_{l=0}^{m_2-1} P\left(\frac{2\pi k}{m_1}, \frac{2\pi l}{m_2}\right) = C_4(q^{\zeta_1} + q^{m_1 - \zeta_1}) \left( s^2 - 2s \cos \frac{2\pi}{m_2} + 1 + \rho(1-s)^2 \cos \frac{2\pi\zeta_1}{m_1} \right), \quad (5)$$

where,  $C_4 = \frac{1-q}{(1-q^{m_1})(1+q)} \left( \frac{q^2 - 2q \cos \frac{2\pi}{m_1} + 1}{(q^2 - 2q \cos \frac{2\pi}{m_1} + 1)(s^2 - 2s \cos \frac{2\pi}{m_2} + 1) + \rho(1-q)^2(1-s)^2} \right)$ .

The distribution given in (5) is symmetric around the direction  $\frac{2\pi\alpha}{m_1}$  and is thus referred to as the “marginal wrapped symmetric geometric” (MWSG) distribution of  $X_1$ . Similarly, the marginal distribution of  $X_2$  is obtained analogously and is symmetric around  $\frac{2\pi\beta}{m_2}$ .

**Theorem 3** For  $\rho \geq 0$ , excluding the cases where  $\{q = s = 1\}$  or  $\{q = 1, \rho = 0\}$ , the MWSG distribution is unimodal with the mode at  $\frac{2\pi\alpha}{m_1}$ .

This implies that for nonnegative  $\rho$ , the distribution is unimodal, except in the specific limiting cases where it reduces to the uniform distribution. These limiting cases are summarized in Table 2.

**Table 2:** Limits of pmf (5) on boundaries of parameter space

$(q, s)$	pmf $P(\cdot)$
$(0, 1) \times \{1\}$	$\left(\frac{1-q}{(1-q^{m_1})(1+q)}\right)(q^{\zeta_1} + q^{m_1-\zeta_1})$
$\{1\} \times (0, 1)$	$\frac{1}{m_1} \left(1 + \rho \left(\frac{(1-s)^2 \cos \frac{2\pi\zeta_1}{m_1}}{s^2 - 2s \cos \frac{2\pi}{m_2} + 1}\right)\right)$
$(0, 1) \times \{0\}$	$C_5 (q^{\zeta_1} + q^{m_1-\zeta_1}) (1 + \rho \cos \frac{2\pi\zeta_1}{m_1}),$ where $C_5 = \left(\frac{(1-q)(q^2 - 2q \cos \frac{2\pi}{m_1} + 1)}{(1-q^{m_1})(1+q)(q^2 - 2q \cos \frac{2\pi}{m_1} + 1) + \rho(1-q)^2}\right)$
$\{0\} \times (0, 1)$	$\begin{cases} 1 & \text{if } k = \alpha \\ 0 & \text{else} \end{cases}$
$\{1\} \times \{1\}$	$\frac{1}{m_1}, \quad \text{for } k \in \mathbf{Z}_{m_1}$

Table 2 summarizes the limiting forms of the pmf on the boundaries of the parameter space of  $(q, s)$ . It highlights how specific parameter combinations lead to simplified distributions, such as degenerate or uniform cases, consistent with the conditions discussed in Theorem 3. The first case in this table, corresponding to  $(q, s) \in (0, 1) \times \{1\}$ , is the WSG distribution.

### 3.2 Conditional wrapped geometric distribution

Here, we derive the conditional distribution of  $X_2$  given  $X_1 = \frac{2\pi k}{m_1}$ , expressed as

$$P\left(\frac{2\pi l}{m_2} \middle| \frac{2\pi k}{m_1}\right) = C_6 \left( \frac{(s^{\zeta_2} + s^{m_2-\zeta_2})(1 + \rho \cos \left(\frac{2\pi\zeta_1}{m_1} - \delta \frac{2\pi\zeta_2}{m_2}\right))}{1 - 2s \cos \frac{2\pi}{m_2} + s^2 + \rho(1-s)^2 \cos \frac{2\pi\zeta_1}{m_1}} \right), \quad (6)$$

where,  $C_6 = \left(\frac{1-s}{(1-s^{m_2})(1+s)}\right)(1 - 2s \cos \frac{2\pi}{m_2} + s^2)$ .

The distribution given in (6) is referred to as the “conditional wrapped geometric” (CWG) distribution. Figure 2 shows how the parameters  $\alpha$ ,  $\beta$ , and  $\rho$  affect the conditional distribution of  $X_2$ , under the settings  $m_1 = m_2 = 10$ ,  $q = s = 0.5$ , and  $\delta = 1$ , given that  $X_1 = 6\pi/m_1$ .

In Figure 2, the case  $\rho = 0$  represents the marginal pmf of  $X_2$ , which is the WSG distribution, since  $X_1$  and  $X_2$  are independent. As evident in Subfigures (a), (c), and (d), as the magnitude of  $\rho$  increases, the conditional distribution becomes asymmetric, reflecting the emergence of dependence. Generally, the dominant mode remains at  $\frac{2\pi\beta}{m_2}$ . However, for specific settings such as  $\rho = -0.9$ ,  $\alpha = 3$ , and  $\beta = 6$  (see subfigure (b)),

it shifts away from this direction, illustrating how the parameters  $\alpha$ ,  $\beta$ , and  $\rho$  jointly influence the shape and asymmetry of the conditional distribution.

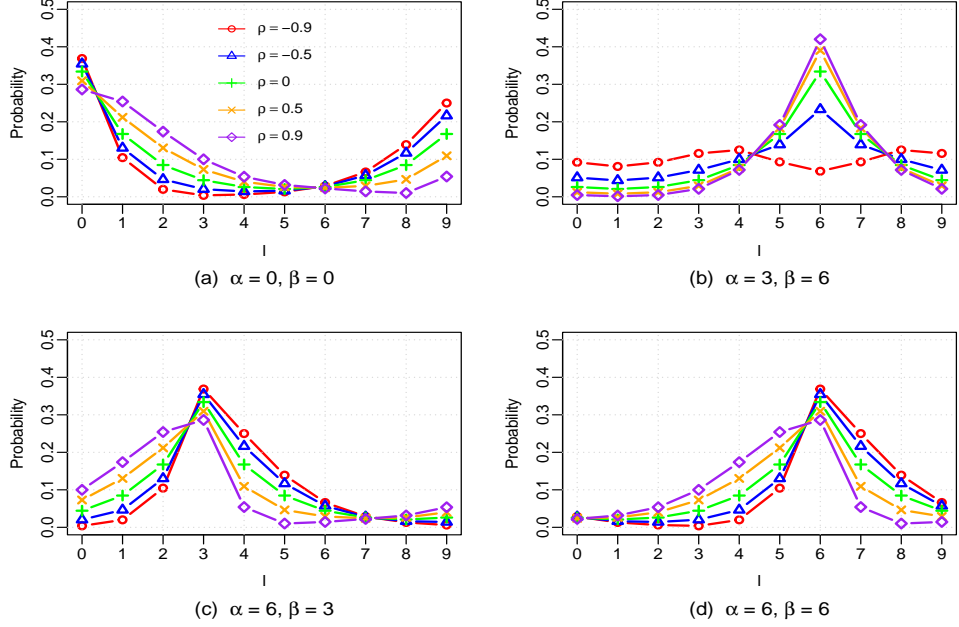


**Fig. 2:** Probability mass plot of CWG distribution for fixed  $X_1 = 6\pi/m_1$

## 4 Generalized BWG distribution

In this section, we generalize the pmf (4) by allowing  $\alpha \in [0, m_1)$  and  $\beta \in [0, m_2)$ . This generalization introduces asymmetry into the distribution, except when  $\alpha$  and  $\beta$  are integers. For  $\rho \geq 0$ , the dominant modes remain in the set  $\left\{ \frac{2\pi[\alpha]}{m_1}, \frac{2\pi[\alpha+1]}{m_1} \right\} \times \left\{ \frac{2\pi[\beta]}{m_2}, \frac{2\pi[\beta+1]}{m_2} \right\}$ , where  $[\cdot]$  denotes the greatest integer function. The generalized form of this pmf is expressed as

$$P\left(\frac{2\pi k}{m_1}, \frac{2\pi l}{m_2}\right) = C_7 (q^{\zeta_1} + q^{m_1 - \zeta_1})(s^{\zeta_2} + s^{m_2 - \zeta_2}) \left(1 + \rho \cos\left(\frac{2\pi\zeta_1}{m_1} - \delta \frac{2\pi\zeta_2}{m_2}\right)\right), \quad (7)$$

where  $C_7$  is the normalizing constant. Its reciprocal is given by

$$\frac{1}{C_7} = \sum_{n_1=0}^{m_1-1} \sum_{n_2=0}^{m_2-1} (q^{n_1+a} + q^{m_1-n_1-a})(s^{n_2+b} + s^{m_2-n_2-b}) \left(1 + \rho \cos\left(\frac{2\pi(n_1+a)}{m_1} - \delta \frac{2\pi(n_2+b)}{m_2}\right)\right)$$

$$= (1 - q^{m_1})(1 - s^{m_2}) \left( \frac{(q^a + q^{1-a})(s^b + s^{1-b})}{(1-q)(1-s)} + \rho \frac{C_8}{(q^2 - 2q \cos \frac{2\pi}{m_1} + 1)(s^2 - 2s \cos \frac{2\pi}{m_2} + 1)} \right),$$

$$\text{where } C_8 = (s^b - s^{2-b}) \left( (q^a - q^{2-a}) \cos \left( \frac{2\pi a}{m_1} - \delta \frac{2\pi b}{m_2} \right) + (q^{1-a} - q^{1+a}) \cos \left( \frac{2\pi(1-a)}{m_1} + \delta \frac{2\pi b}{m_2} \right) \right) \\ + (s^{1-b} - s^{1+b}) \left( (q^a - q^{2-a}) \cos \left( \frac{2\pi a}{m_1} + \delta \frac{2\pi(1-b)}{m_2} \right) + (q^{1-a} - q^{1+a}) \cos \left( \frac{2\pi(1-a)}{m_1} - \delta \frac{2\pi(1-a)}{m_2} \right) \right).$$

The distribution given in (7) is referred to as the “bivariate generalized wrapped geometric” (BGWG) distribution. The quantities  $a$  and  $b$  appearing in the normalizing constant  $C_7$  represent the fractional parts of  $\alpha$  and  $\beta$ , respectively.

**Corollary 2** *In the BGWG distribution, the random variables  $X_1$  and  $X_2$  are independent when  $\rho = 0$ .*

This result mirrors the independence property of the BWG distribution, confirming that the generalization preserves this structural characteristic.

## 5 Measuring dependence using $\rho$

Since Corollary 1 and Corollary 2 establish that the random variables  $X_1$  and  $X_2$  are independent when  $\rho = 0$ , this motivates an examination of the role of  $\rho$  in their dependence structure. In a bivariate directional framework, interdependence between circular random variables is typically quantified through a correlation coefficient. Accordingly, we derive a relationship between  $\rho$  and an appropriate correlation coefficient for the circular random variables  $X_1$  and  $X_2$ .

Jupp and Mardia [12] proposed a correlation coefficient for the bivariate circular case by embedding the circular variables  $X_1$  and  $X_2$  into the Euclidean plane. Specifically, each variable is defined as  $t'_1(X_1) = (\cos X_1, \sin X_1)$  and  $t'_2(X_2) = (\cos X_2, \sin X_2)$ . The covariance matrix of the joint vector  $(t'_1(X_1), t'_2(X_2))$  is given by

$$\Sigma = \begin{bmatrix} \Sigma_{11} & \Sigma_{12} \\ \Sigma_{21} & \Sigma_{22} \end{bmatrix},$$

and the correlation coefficient is defined as  $\rho_1^2 = \text{tr}(\Sigma_{11}^{-1} \Sigma_{12} \Sigma_{22}^{-1} \Sigma_{21})$ . An explicit expression for  $\rho_1^2$  is given by

$$\rho_1^2 = \{ \rho_{1cc}^2 + \rho_{1cs}^2 + \rho_{1sc}^2 + \rho_{1ss}^2 + 2(\rho_{1cc}\rho_{1ss} + \rho_{1cs}\rho_{1sc})\rho'_1\rho'_2 - 2(\rho_{1cc}\rho_{1sc} + \rho_{1cs}\rho_{1ss})\rho'_1 - 2(\rho_{1cc}\rho_{1cs} + \rho_{1sc}\rho_{1ss})\rho'_2 \} / \{ (1 - \rho'_1)^2(1 - \rho'_2)^2 \}, \quad (8)$$

where  $\rho_{1cc} = \text{corr}(\cos X_1, \cos X_2)$ ,  $\rho_{1cs} = \text{corr}(\cos X_1, \sin X_2)$ , etc., and  $\rho'_1 = \text{corr}(\cos X_1, \sin X_1)$ ,  $\rho'_2 = \text{corr}(\cos X_2, \sin X_2)$ , and  $\text{corr}(\cdot, \cdot)$  denotes the usual correlation coefficient.

**Theorem 4** *For the BWG distribution, if  $\rho > 0$ , then the correlation coefficient  $\rho_1^2$  is monotonically increasing in  $\rho$ , and if  $\rho < 0$ , then it is monotonically decreasing in  $\rho$ .*

*Remark 1* For the BGWG distribution, if  $\rho > 0$ , then the correlation coefficient  $\rho_1^2$  is monotonically increasing in  $\rho$ , and if  $\rho < 0$ , then it is monotonically decreasing in  $\rho$ . (This property is verified for  $m_1, m_2 \leq 600$ ; details in the supplement.)

These results indicate that the parameter  $\rho$  governs the strength of dependence between  $X_1$  and  $X_2$ . Larger absolute values of  $\rho$  correspond to stronger association, while its sign determines the direction of dependence. Thus,  $\rho$  serves as a natural dependence parameter for the BWG and BGWG distributions.

### 5.1 Interpretation of $\rho$ in BWG and BGWG distributions

According to Theorem 4 and Remark 1, for the BWG and BGWG distributions, the parameter  $\rho$  is directly related to the correlation coefficient  $\rho_1^2$ .

For  $\rho > 0$ , the type of dependence is determined by  $\delta$ :

- If  $\delta = 1$ ,  $X_1$  and  $X_2$  exhibit a rotational dependence, meaning they move in the same direction, either clockwise or anticlockwise, relative to their mean directions together.
- If  $\delta = -1$ ,  $X_1$  and  $X_2$  exhibit an anti-rotational dependence, meaning they move in the opposite directions, one clockwise and another anticlockwise, relative to their mean directions together.

For  $\rho = 0$ , no rotational dependence exists; in fact, they are independent. When  $\rho < 0$ , the variables exhibit dependence, but this cannot be explicitly stated in terms of rotational or anti-rotational dependence.

## 6 Simulation study

This section presents simulation studies conducted for the BWG and BGWG distributions. Throughout the study, we fix  $m_1 = 5$  and  $m_2 = 6$ , and consider two distinct parameter configurations under three different sample sizes. The bivariate random samples were generated sequentially by sampling  $X_1$  from its marginal distribution and subsequently sampling  $X_2$  from the conditional distribution of  $X_2$  given  $X_1$ . Since the parameters are of mixed type (discrete and continuous) in both distributions, parameter estimation is performed in two steps.

For the BWG distribution,

- In the first step, each combination  $(\delta, \alpha, \beta) \in \{-1, 1\} \times \mathbf{Z}_{m_1} \times \mathbf{Z}_{m_2}$  is substituted into the log-likelihood function, yielding  $2 \times m_1 \times m_2$  likelihood functions, each involving three continuous parameters.
- In the second step, each of these log-likelihood functions is maximized with respect to the continuous parameters, and the final estimates are obtained by selecting the combination of  $(\delta, \alpha, \beta)$  and continuous parameters that produces the highest log-likelihood value.

For the BGWG distribution, which involves one discrete parameter  $\delta$  (with the remaining parameters being continuous), we follow the same steps as for the BWG. The results are summarized below.

**Results and discussion:** The results are based on 1,000 independent simulations. Table 3 and Table 4 present the results for the BWG and BGWG distributions, respectively.

The standard errors reported in these tables represent the sample standard deviation of the 1,000 parameter estimates obtained from the simulations. Additionally, we summarize the estimates of the discrete parameters based on their frequencies across all simulations in the last columns of these tables.

**Table 3:** Estimates (with Standard Error in parentheses) for BWG

Sample size		MLE (Standard Error)					
n		$\hat{q}_{MLE}$	$\hat{s}_{MLE}$	$\hat{\rho}_{MLE}$	$\hat{\alpha}$	$\hat{\beta}$	$\hat{\delta}$
True value		$q = 0.2$	$s = 0.3$	$\rho = -0.5$	$\alpha = 0$	$\beta = 0$	$\delta = 1$
50		0.203 (0.059 )	0.299 (0.078)	-0.453 (0.324)	(1000,0,0,0,0)	(998,1,0,0,0,1)	(187,813)
200		0.201 (0.027 )	0.300 (0.036)	-0.493 ( 0.132)	(1000,0,0,0,0)	(1000,0,0,0,0,0)	(19,981)
500		0.200 ( 0.017 )	0.300 (0.022)	-0.495 (0.077)	(1000,0,0,0,0)	(1000,0,0,0,0,0)	(0,1000)
True value		$q = 0.6$	$s = 0.7$	$\rho = 0.8$	$\alpha = 2$	$\beta = 2$	$\delta = -1$
50		0.638 ( 0.165 )	0.692 (0.117)	0.411 (0.709)	(33,61,796,65,45)	(22,63,712,62,24,117)	(993,7)
200		0.606 (0.066)	0.705 ( 0.069 )	0.763 ( 0.246 )	(1,1,995,2,1 )	(1,2,977,1,1,18 )	(1000,0)
500		0.600 ( 0.037 )	0.704 (0.043)	0.801 (0.047)	(0,0,1000,0,0,0)	(0,0,1000,0,0,0)	(1000,0)

**Table 4:** Estimates (with Standard Error in parentheses) for BGWG

Sample size		MLE (Standard Error)					
n		$\hat{q}_{MLE}$	$\hat{s}_{MLE}$	$\hat{\rho}_{MLE}$	$\hat{\alpha}$	$\hat{\beta}$	$\hat{\delta}$
True value		$q = 0.2$	$s = 0.3$	$\rho = -0.5$	$\alpha = 2$	$\beta = 3$	$\delta = 1$
50		0.175 (0.057 )	0.276 ( 0.080 )	-0.476 ( 0.327 )	1.999 ( 0.137 )	3.002 (0.173)	(185, 815)
200		0.1888 (0.027 )	0.2873 (0.035)	-0.4981 ( 0.119 )	2.0041 (0.070)	2.9943 (0.091)	(8, 992)
500		0.193 ( 0.018 )	0.293 ( 0.022 )	-0.494 (0.074)	1.997 (0.047)	2.999 (0.057)	(0,1000)
True value		$q = 0.6$	$s = 0.7$	$\rho = 0.8$	$\alpha = 3$	$\beta = 2$	$\delta = -1$
50		0.558 (0.133 )	0.667 (0.130)	0.330 (0.769)	2.869 (0.740)	2.482 (1.229)	(989, 11)
200		0.585 (0.070 )	0.692 ( 0.074 )	0.756 ( 0.289 )	2.988 ( 0.249 )	2.074 (0.494)	(1000, 0)
500		0.589 ( 0.040 )	0.693 (0.044)	0.800 ( 0.087 )	2.996 ( 0.118 )	2.011 (0.192)	(1000,0)

From Table 3 and Table 4, it is clearly seen that as the sample size increases, the estimates become more accurate. The estimation accuracy of the discrete parameters  $\alpha$  and  $\beta$ , as presented in Table 3, is notably higher for lower values of parameters  $q$  and  $s$  (e.g.,  $q = 0.2, s = 0.3$ ) compared to larger values (e.g.,  $q = 0.6, s = 0.7$ ). This behavior occurs because

smaller values of  $q$  and  $s$  lead to a stronger concentration of the BWG distribution around the location  $(\frac{2\pi\alpha}{m_1}, \frac{2\pi\beta}{m_2})$ ; in fact, when  $q = 0$  and  $s = 0$ , the distribution degenerates exactly at this location. Conversely, as  $q$  and  $s$  approach 1, the distribution becomes flatter and nearly uniform (limiting cases discussed in Table 1), resulting in greater estimation variability.

Furthermore, the estimation accuracy of the discrete parameter  $\delta$ , presented in Table 3 and Table 4, is highly affected by the parameter  $\rho$ . Specifically, the accuracy is higher for large absolute values of  $\rho$  (e.g.,  $|\rho| = 0.8$ ) compared to lower absolute values (e.g.,  $|\rho| = 0.5$ ). This behavior occurs because the role of  $\delta$  in the distributions is governed by the term  $\rho \cos\left(\frac{2\pi\xi_1}{m_1} - \delta\frac{2\pi\xi_2}{m_2}\right)$ , and the influence of this term in both distributions directly depends on  $|\rho|$ . Consequently, as  $|\rho|$  decreases, the distinguishability between  $\delta = 1$  and  $\delta = -1$  diminishes.

## 7 Data analysis

In this section, we apply the proposed method to study the dependence structure of wind directions across different stations in India. Data were recorded from three stations: Gwalior (located in North-Central India), Chennai (on the southeastern coast), and Mangaluru (on the southwestern coast). The observations corresponding to periods of calm (no wind) were excluded from the analysis.

The wind directions were recorded as inherently discrete circular variables taking values in sixteen compass directions (e.g., N, NNE, NE). These compass directions were mapped to sixteen integers 0, 1, ..., 15, and Figure 3 presents the mapping from these wind directions to their corresponding integers. Since the analysis considers pairwise observations of wind directions at two different stations, we set  $m_1 = m_2 = 16$  for consistency. The model parameters were estimated using maximum likelihood estimation (MLE).

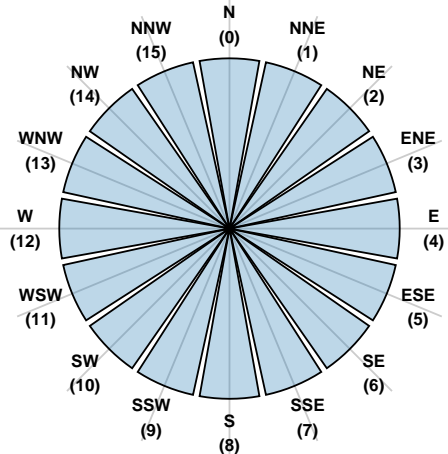


**Fig. 3:** Representation of the directions

## 7.1 Dataset-I

*Dataset-I* is constructed from wind direction data collected at two locations: Gwalior Fort in Gwalior and Rao Circle in Mangaluru, during the period from 24 December 2024 to 7 January 2025. Table 5 presents the contingency table for this dataset.

We fitted the proposed BGWG distribution to *Dataset-I*, and the estimated parameters are provided in Table 6. Figure 4 displays the heatmap of the estimated pmf.

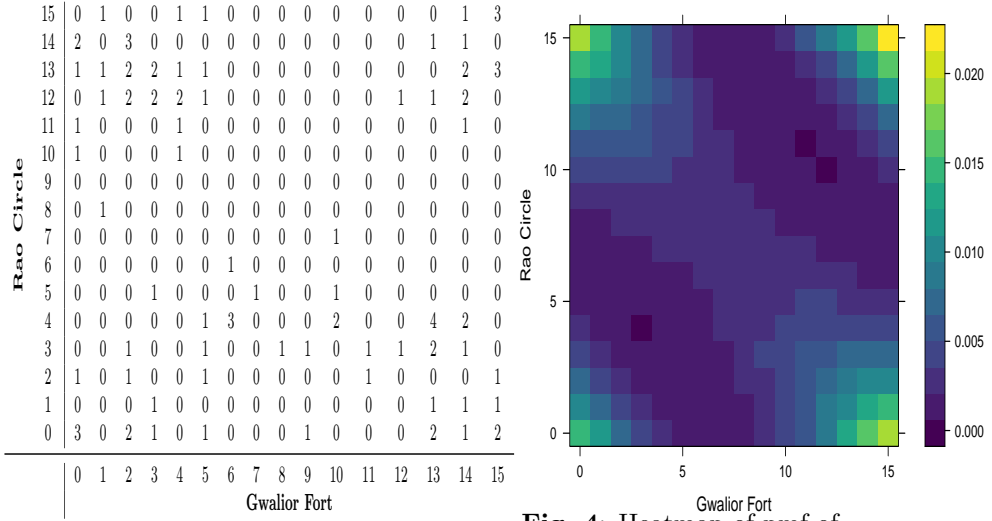


**Table 5:** Contingency table of *Dataset-I*

**Fig. 4:** Heatmap of pmf of estimated BGWG

**Table 6:** Estimated parameters of the BGWG for *Dataset-I*

Parameters	Estimates (Standard Error)
$\hat{\alpha}_{MLE}$	15.138 (0.484)
$\hat{\beta}_{MLE}$	15.249 (0.452)
$\hat{q}_{MLE}$	0.814 (0.044)
$\hat{s}_{MLE}$	0.794 (0.043)
$\hat{\rho}_{MLE}$	0.804 (0.123)
$\hat{\delta}_{MLE}$	-1
AIC	977.573

**Interpretation:** The estimates  $\hat{\rho}_{MLE} = 0.804$  and  $\hat{\delta}_{MLE} = -1$  suggest an anti-rotational dependence between the wind directions at Gwalior Fort in Gwalior, and Rao Circle in Mangaluru.

We compare the performance of the BGWG distribution with discretized versions of prominent continuous distributions. The Akaike information criterion (AIC) values are

978.609 for the wrapped Cauchy model, 976.045 for the von Mises Sine model, and 992.434 for the von Mises Cosine model. The AIC was computed using the formula  $AIC = 2\mathcal{P} + 2\mathcal{L}$ , where  $\mathcal{P}$  denotes the number of parameters and  $\mathcal{L}$  denotes the negative log-likelihood value.

## 7.2 Dataset-II

*Dataset-II* was obtained from wind direction observations recorded at two locations: Marina Beach in Chennai and Gwalior Fort in Gwalior, India, during the period 22 December 2024 to 7 January 2025. Table 7 provides the contingency table for this dataset.

We fitted the BGWG distribution to *Dataset-II*, and the estimated parameters are given in Table 8. Figure 5 shows the heatmap of the estimated pmf.

	0	1	2	3	4	5	6	7	8	9	10	11	12	13	14	15
Gwalior Fort	15	0	1	8	1	0	0	0	0	0	0	0	0	0	0	0
	14	1	8	3	0	0	0	0	0	0	0	0	0	0	0	0
	13	0	5	6	1	0	0	0	0	0	0	0	0	0	0	0
	12	0	1	1	0	0	0	0	0	0	0	0	0	0	0	0
	11	0	0	2	0	0	0	0	0	0	0	0	0	0	0	0
	10	0	1	3	0	0	0	0	0	0	0	0	0	0	0	1
	9	0	0	2	0	0	0	0	0	0	0	0	0	0	0	0
	8	1	1	0	1	0	0	0	0	0	0	0	0	0	0	0
	7	0	1	0	0	0	0	0	0	0	0	0	0	0	0	0
	6	1	4	0	2	0	0	0	0	0	0	0	0	0	0	0
	5	1	2	4	1	0	0	0	0	0	0	0	0	0	0	2
	4	2	1	2	2	0	0	0	0	0	0	0	0	0	0	0
	3	2	2	1	1	0	0	0	0	0	0	0	0	0	0	2
	2	5	2	0	0	0	0	0	0	0	0	0	0	0	0	4
	1	2	1	2	0	0	0	0	0	0	0	0	0	0	0	0
	0	1	3	5	0	0	0	0	0	0	0	0	0	0	0	0

Table 7: Contingency table of *Dataset-II*

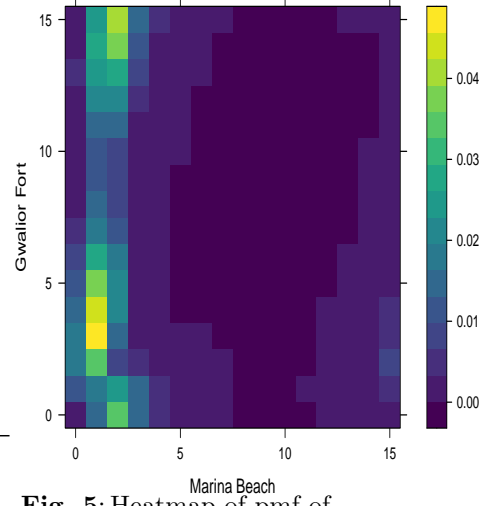


Fig. 5: Heatmap of pmf of estimated BGWG

Table 8: Estimated parameters of BGWG for *Dataset-II*

Parameters	Estimates (Sd Error)
$\hat{\alpha}_{MLE}$	1.421 (0.069)
$\hat{\beta}_{MLE}$	1.159 (0.230)
$\hat{q}_{MLE}$	0.218 (0.030)
$\hat{s}_{MLE}$	0.549 (0.032)
$\hat{\rho}_{MLE}$	-0.945 (0.036)
$\hat{\delta}_{MLE}$	1
AIC	892.961

**Interpretation:** The estimate  $\hat{\rho}_{MLE} = -0.945$  suggests a strong dependence between the wind directions at Marina Beach, Chennai, and Gwalior Fort.

For comparison, the AIC values of the discretized bivariate distributions are 921.386 for the wrapped Cauchy model, 889.110 for the von Mises Sine model, and 889.920 for the von Mises Cosine model.

### 7.3 Dataset-III

*Dataset-III* is constructed from wind direction data collected at two locations: Marina Beach in Chennai and Rao Circle in Mangaluru, during the period from 24 December 2024 to 7 January 2025. Table 9 presents the contingency table for this dataset.

We fitted the BGWG distribution to *Dataset-III*, and the estimated parameters are given in Table 10. Figure 6 shows the heatmap of the estimated pmf.

15	1	2	4	1	0	0	0	0	0	0	0	0	0	0	0	0
14	2	2	2	0	0	0	0	0	0	0	0	0	0	0	0	1
13	2	2	7	1	0	0	0	0	0	0	0	0	0	0	0	1
12	3	1	6	1	0	0	0	0	0	0	0	0	0	0	0	1
11	1	1	1	0	0	0	0	0	0	0	0	0	0	0	0	0
10	0	0	1	1	0	0	0	0	0	0	0	0	0	0	0	0
9	0	0	0	0	0	0	0	0	0	0	0	0	0	0	0	0
8	0	0	1	0	0	0	0	0	0	0	0	0	0	0	0	0
7	0	0	1	0	0	0	0	0	0	0	0	0	0	0	0	0
6	0	0	0	1	0	0	0	0	0	0	0	0	0	0	0	0
5	1	1	1	0	0	0	0	0	0	0	0	0	0	0	0	0
4	0	7	3	3	0	0	0	0	0	0	0	0	0	0	0	1
3	0	6	5	0	0	0	0	0	0	0	0	0	0	0	0	0
2	0	1	3	1	0	0	0	0	0	0	0	0	0	0	0	1
1	1	2	1	0	0	0	0	0	0	0	0	0	0	0	0	0
0	2	3	5	1	0	0	0	0	0	0	0	0	0	0	0	2

Table 9: Contingency table of *Dataset-III*

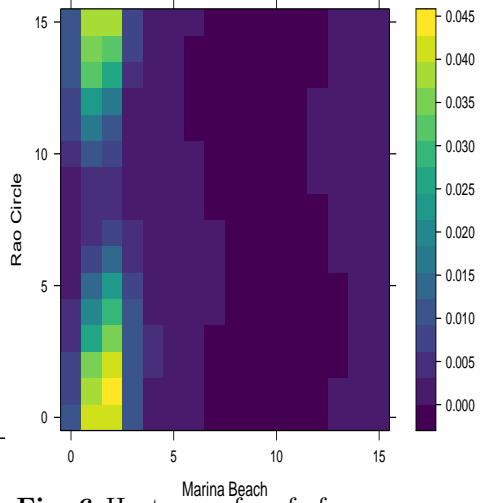


Fig. 6: Heatmap of pmf of estimated BGWG

**Interpretation:** The estimate  $\hat{\rho}_{MLE} = -0.834$  suggests a strong dependence between the wind directions at Marina Beach in Chennai, and Rao Circle in Mangaluru.

For comparison, the AIC values of the discretized bivariate distributions are 851.526 for the wrapped Cauchy model, 822.844 for the von Mises Sine model, and 822.986 for the von Mises Cosine model.

Goodness-of-fit tests were conducted for all datasets using Pearson's chi-square statistic, and the corresponding results are provided in the supplement. The datasets were also analyzed using the BWG distribution, with detailed findings included in the supplement.

Overall, the proposed methods provide a direct and computationally efficient framework for analyzing bivariate ordinal circular data, producing results that are comparable to or better than those obtained from discretized versions of traditional models. Moreover, this

approach effectively eliminates the approximation errors and heavy computational demands associated with discretization.

**Table 10:** Estimated parameters of BGWG for *Dataset-III*

Parameters	Estimates (Sd Error)
$\hat{\alpha}_{MLE}$	1.523 (0.077)
$\hat{\beta}_{MLE}$	8.265 (0.377)
$\hat{q}_{MLE}$	0.272 ( 0.038)
$\hat{s}_{MLE}$	0.990 ( 0.121)
$\hat{\rho}_{MLE}$	-0.834 (0.101)
$\hat{\delta}_{MLE}$	1
AIC	824.418

## 8 Conclusion

This study addresses the challenges associated with modeling bivariate ordinal circular random variables. We proposed new models defined on the discrete torus and examined how their parameters influence the underlying dependence structure. The performance of these models was evaluated using three bivariate wind direction datasets and compared with the discretized versions of well-known existing models. The proposed framework can also be applied to analyze how wave directions at one location correlate with those at other locations in the ocean, with potential applications in areas such as animal movement, traffic flow, and seismic activity.

Using the proposed bivariate models, we analyzed the joint wind direction observations from pairs of meteorological stations. Our findings demonstrate a significant relationship between the wind directions at these stations, even though they are geographically distant, possibly reflecting the effect of the geography of the Indian subcontinent. In future, multi-variate extensions could be constructed using copula-based frameworks to link the proposed discrete circular marginals with continuous linear variables such as wind speed and temperature. Furthermore, time-series analysis offers a natural generalization of the proposed framework, potentially utilizing Hidden Markov Models to capture temporal dependence.

## Declarations

### Funding

This project is partially funded by the Government of India as part of the Start-up Research Grant. The funding is provided through the Science of Engineering Board of the Department of Science and Technology to Dr. Jayant Jha (SRG/2022/000151). Brajesh Kumar Dhakad supported by the National Board for Higher Mathematics (NBHM) (0203/4/2022/R&D-II/3262). The funders had no role in the methodological development, data analysis, decision to publish, or preparation of the manuscript.

### Competing Interests

The authors have no relevant financial or non-financial interests to disclose.

### Data Availability

The data supporting the findings of this study are available from the corresponding author upon request.

### Code Availability

The R code used for the simulations and data analysis is available from the corresponding author upon request.

## Appendix A Proof of Theorem 1

From equation (3), the reciprocal of  $C_1$  is obtained as follows:

$$\begin{aligned} \frac{1}{C_1} &= \sum_{k=0}^{m_1-1} \sum_{l=0}^{m_2-1} (q^{\zeta_1} + q^{m_1-\zeta_1})(s^{\zeta_2} + s^{m_2-\zeta_2}) \left( 1 + \rho \cos \left( \frac{2\pi\zeta_1}{m_1} - \delta \frac{2\pi\zeta_2}{m_2} \right) \right) \\ &= (1 - q^{m_1})(1 - s^{m_2})(1 + q)(1 + s) \left( \frac{1}{(1 - s)(1 - q)} + \rho \frac{(1 - q)(1 - s)}{(q^2 - 2q \cos \frac{2\pi}{m_1} + 1)(s^2 - 2s \cos \frac{2\pi}{m_2} + 1)} \right). \end{aligned}$$

The closed-form expression of the double sum is obtained by first expressing  $\cos(\cdot)$  in terms of exponential functions using Euler's formula, and then applying the finite geometric series.

The function (4) is non-negative and its values sum to one; hence it serves as the pmf of  $(X_1, X_2)$ .

## Appendix B Proof of Corollary 1

From Theorem 1, if  $\rho = 0$ , then the joint pmf given in (4) takes the following form:

$$P\left(\frac{2\pi k}{m_1}, \frac{2\pi l}{m_2}\right) = \left( \frac{(1 - q)(1 - s)}{(1 - q^{m_1})(1 - s^{m_2})(1 + q)(1 + s)} \right) (q^{\zeta_1} + q^{m_1-\zeta_1})(s^{\zeta_2} + s^{m_2-\zeta_2}). \quad (\text{B1})$$

The marginal pmf of  $X_1$  is obtained by summing the pmf in (B1) over the values  $\frac{2\pi l}{m}$ , where  $l \in \mathbf{Z}_{\mathbf{m}_2}$ , and is given by:

$$P\left(\frac{2\pi k}{m_1}\right) = \left( \frac{1 - q}{(1 - q^{m_1})(1 + q)} \right) (q^{\zeta_1} + q^{m_2-\zeta_1}). \quad (\text{B2})$$

Similarly, the marginal pmf of  $X_2$  can be derived, and it is given by:

$$P\left(\frac{2\pi l}{m_2}\right) = \left( \frac{1 - s}{(1 - s^{m_2})(1 + s)} \right) (s^{\zeta_2} + s^{m_2-\zeta_2}). \quad (\text{B3})$$

Hence, the joint pmf in (B1) factorizes into the product of the marginals given in (B2) and (B3).

## Appendix C Proof of Theorem 2

Let  $f_1(k) = (q^{\zeta_1} + q^{m_1-\zeta_1})$ ,  $f_2(l) = (s^{\zeta_2} + s^{m_2-\zeta_2})$ ,  $f_3\left(\frac{2\pi k}{m_1}, \frac{2\pi l}{m_2}\right) = f_1(k)f_2(l)(1 + \rho \cos(\cdot))$ , and  $f(x) = a^x + a^{m-x}$ ,  $x \in [0, m]$ , where,  $a \in (0, 1)$ ,  $m \in \mathbf{Z}_+$  are constants. Then,

$$f(x) - f(0) = (a^x - 1)(1 - a^{m-x}) < 0, \quad \forall x \in (0, m). \quad (\text{C4})$$

This implies that  $f(x) < f(0)$ . Furthermore, it follows that

$$f_1(k) < f_1(\alpha), \quad \forall k \in \mathbf{Z}_{\mathbf{m}_1}/\{\alpha\} \quad \text{and} \quad f_2(l) < f_2(\beta), \quad \forall l \in \mathbf{Z}_{\mathbf{m}_2}/\{\beta\}. \quad (\text{C5})$$

From equation (C5), if  $\rho \geq 0$ . Then  $\forall (k, l) \in \mathbf{Z}_{\mathbf{m}_1} \times \mathbf{Z}_{\mathbf{m}_2}/\{(\alpha, \beta)\}$ ,

$$f_3\left(\frac{2\pi k}{m_1}, \frac{2\pi l}{m_2}\right) < f_1(\alpha)f_2(\beta) \left( 1 + \rho \cos \left( \frac{2\pi\zeta_1}{m_1} - \delta \frac{2\pi\zeta_2}{m_2} \right) \right) \leq f_3\left(\frac{2\pi\alpha}{m_1}, \frac{2\pi\beta}{m_2}\right), \quad (\text{C6})$$

which implies that  $f_3\left(\frac{2\pi\alpha}{m_1}, \frac{2\pi\beta}{m_2}\right)$  is the highest value of  $f_3(\cdot)$ . Therefore, from equation (C6) and the pmf given in (4), the BWG distribution has a dominant mode at the unique location  $(\frac{2\pi\alpha}{m_1}, \frac{2\pi\beta}{m_2})$ .

## Appendix D Proof of Theorem 3

If  $q = 0$ , then the MWSG distribution degenerates on  $\frac{2\pi\alpha}{m_1}$ . If  $q \neq 0$ , we take  $\alpha = 0$  without loss of generality. For  $m_1 - k > k + 1$ ,

$$(q^k + q^{m_1-k}) \cos \frac{2\pi k}{m_1} \geq (q^{k+1} + q^{m_1-k-1}) \cos \frac{2\pi(k+1)}{m_1}, \quad (\text{D7})$$

and for  $m_1 - k \leq k + 1$ ,

$$(q^k + q^{m_1-k}) \cos \frac{2\pi k}{m_1} \leq (q^{k+1} + q^{m_1-k-1}) \cos \frac{2\pi(k+1)}{m_1}. \quad (\text{D8})$$

From the pmf given in (5), for  $\rho \geq 0$ ,

$$P\left(\frac{2\pi k}{m_1}\right) \geq P\left(\frac{2\pi(k+1)}{m_1}\right), \quad \text{for } k > \frac{m_1-1}{2}, \quad (\text{D9})$$

$$P\left(\frac{2\pi k}{m_1}\right) \leq P\left(\frac{2\pi(k+1)}{m_1}\right), \quad \text{for } k \leq \frac{m_1-1}{2}. \quad (\text{D10})$$

Except for the cases  $\{q = s = 1\}$  and  $\{q = 1, \rho = 0\}$ , the inequalities given in (D9) and (D10) hold strictly. This implies that if the parameters do not satisfy these conditions, then the pmf given in (5) is unimodal, and the mode occurs at  $\left(\frac{2\pi\alpha}{m_1}\right)$ .

## Appendix E Proof of Corollary 2

The proof is analogous to that of Corollary 1.

## Appendix F Proof of Theorem 4

The proof is carried out by examining the two cases  $\delta = 1$  and  $\delta = -1$ . We first consider the case  $\delta = 1$ . We set  $\alpha = 0$  and  $\beta = 0$  without loss of generality to simplify the computation of  $\rho_1^2$ . Under this assumption, the covariances between  $\cos X_1$  and  $\sin X_2$ ,  $\sin X_1$  and  $\cos X_2$ , and  $\cos X_2$  and  $\sin X_2$  are all zero. Consequently,  $\rho_{1cs}$ ,  $\rho_{2sc}$ , and  $\rho_2'$  also vanish, and  $\rho_1^2$  reduces to the following simplified form:

$$\rho_1^2 = \rho_{1cc}^2 + \rho_{1ss}^2. \quad (\text{F11})$$

We next compute  $\rho_{1cc}^2$  and  $\rho_{1ss}^2$  using the correlation formulas  $\frac{\text{cov}(\cos X_1, \cos X_2)^2}{\text{var}(\cos X_1) \text{var}(\cos X_2)}$  and  $\frac{\text{cov}(\sin X_1, \sin X_2)^2}{\text{var}(\sin X_1) \text{var}(\sin X_2)}$ , respectively, where  $\text{var}(\cdot)$  denotes variance and  $\text{cov}(\cdot)$  denotes covariance. Consequently, we obtain the following expressions

$$\begin{aligned}
\text{var}(\sin X_1) &= \frac{1}{2}(1-q)A_1H_1 \left( B_1 \left( \frac{1}{1-q} - \frac{1-q}{A_2} \right) + (1-q)(1-s)^2 \left( \frac{1}{A_1} - \frac{1}{2} \left( \frac{1}{A_3} + \frac{1}{A_1} \right) \right) \rho \right), \\
\text{var}(\sin X_2) &= \frac{1}{2}(1-s)B_1H \left( A_1 \left( \frac{1}{1-s} - \frac{1-s}{B_2} \right) + (1-q)^2(1-s) \left( \frac{1}{B_1} - \frac{1}{2} \left( \frac{1}{B_3} + \frac{1}{B_1} \right) \right) \rho \right), \\
\text{var}(\cos X_1) &= (1-q)A_1H^2 \left( \frac{A_1B_1^2}{2} \left( \frac{1}{1-q} + \frac{1-q}{A_2} \right) - \frac{B_1^2(1-q)^3}{A_1} + \left( \frac{A_1B_1(1-q)(1-s)^2}{4} \left( \frac{1}{A_3} + \frac{3}{A_1} \right) - \frac{B_1(1-q)^2}{2} \right. \right. \\
&\quad \left. \left. (1-s)^2 \left( \frac{1}{1-q} + \frac{1-q}{A_2} \right) \right) \rho - \frac{1}{4} \left( A_1(1-q)(1-s)^4 \left( \frac{1}{1-q} + \frac{1-q}{A_2} \right)^2 - (1-q)^3(1-s)^4 \left( \frac{1}{A_3} + \frac{3}{A_1} \right) \right) \rho^2 \right), \\
\text{var}(\cos X_2) &= (1-s)B_1H^2 \left( \frac{A_1^2B_1}{2} \left( \frac{1}{1-s} + \frac{1-s}{B_2} \right) - \frac{A_1^2(1-s)^3}{B_1} + \left( \frac{A_1B_1(1-q)^2(1-s)}{4} \left( \frac{1}{B_3} + \frac{3}{B_1} \right) - \frac{A_1(1-s)^2}{2} \right. \right. \\
&\quad \left. \left. (1-q)^2 \left( \frac{1}{1-s} + \frac{1-s}{B_2} \right) \right) \rho - \frac{1}{4} \left( B_1(1-q)^4(1-s) \left( \frac{1}{1-s} + \frac{1-s}{B_2} \right)^2 - (1-q)^4(1-s)^3 \left( \frac{1}{B_3} + \frac{3}{B_1} \right) \right) \rho^2 \right), \\
\text{cov}(\sin X_1, \sin X_2) &= \frac{1}{4}(1-q)(1-s)A_1B_1H \left( \frac{1-s}{B_2} - \frac{1}{1-s} \right) \left( \frac{1-q}{A_2} - \frac{1}{1-q} \right) \rho, \\
\text{cov}(\cos X_1, \cos X_2) &= (1-q)(1-s)H^2 \left( \frac{A_1^2}{2} \left( \frac{1}{1-q} + \frac{1-q}{A_2} \right) - (1-q)^3 \right) \left( \frac{B_1^2}{2} \left( \frac{1}{1-s} + \frac{1-s}{B_2} \right) - (1-s)^3 \right) \rho,
\end{aligned}$$

where  $\frac{1}{H} = A_1B_1 + \rho(1-q)^2(1-s)^2$ ,  $A_i = 1 + q^2 - 2q \cos \frac{2i\pi}{m_1}$ ,  $B_i = 1 + s^2 - 2s \sin \frac{2i\pi}{m_2}$ , for  $i \in \{1, 2, 3\}$ . Therefore, these expressions are used to calculate  $\rho_1^2$  for BWG distribution. Let  $f(\rho) = \rho_{1ss}^2$  and  $g(\rho) = \rho_{1cc}^2$ . Then,

$$f(\rho) = \frac{\alpha_3\rho^2}{(B_1\alpha_1 + \alpha_4\rho)(A_1\alpha_2 + \alpha_5\rho)}, \quad (\text{F12})$$

where  $\alpha_1 = \left( \frac{1}{1-q} - \frac{1-q}{A_2} \right)$ ,  $\alpha_2 = \left( \frac{1}{1-s} - \frac{1-s}{B_2} \right)$ ,  $\alpha_3 = \frac{1}{4}(1-q)(1-s)A_1B_1\alpha_1^2\alpha_2^2$ ,  $\alpha_4 = (1-q)(1-s)^2 \left( \frac{1}{A_1} - \frac{1}{2} \left( \frac{1}{A_3} + \frac{1}{A_1} \right) \right)$ ,  $\alpha_5 = (1-q)^2(1-s) \left( \frac{1}{B_1} - \frac{1}{2} \left( \frac{1}{B_3} + \frac{1}{B_1} \right) \right)$ , and

$$g(\rho) = \frac{(1-q)(1-s)A_1B_1\beta_1^2\beta_2^2\rho^2}{(B_1^2\beta_1 + \beta_3\rho - \beta_5\rho^2)(A_1^2\beta_2 + \beta_4\rho - \beta_6\rho^2)}, \quad (\text{F13})$$

where  $\beta_1 = \frac{A_1}{2} \left( \frac{1}{1-q} + \frac{1-q}{A_2} \right) - \frac{(1-q)^3}{A_1}$ ,  $\beta_2 = \frac{B_1}{2} \left( \frac{1}{1-s} + \frac{1-s}{B_2} \right) - \frac{(1-s)^3}{B_1}$ ,  $\beta_3 = \frac{B_1}{2}(1-q)(1-s)^2 \left( \frac{A_1}{2} \left( \frac{1}{A_3} + \frac{3}{A_1} \right) - (1-q) \left( \frac{1}{1-q} + \frac{1-q}{A_2} \right) \right)$ ,  $\beta_4 = \frac{A_1}{2}(1-q)^2(1-s) \left( \frac{B_1}{2} \left( \frac{1}{B_3} + \frac{3}{B_1} \right) - (1-s) \left( \frac{1}{1-s} + \frac{1-s}{B_2} \right) \right)$ ,  $\beta_5 = \frac{1}{4}(1-q)(1-s)^4 \left( A_1 \left( \frac{1}{1-q} + \frac{1-q}{A_2} \right)^2 - (1-q)^2 \left( \frac{1}{A_3} + \frac{3}{A_1} \right) \right)$ ,  $\beta_6 = \frac{1}{4}(1-q)^4(1-s) \left( B_1 \left( \frac{1}{1-s} + \frac{1-s}{B_2} \right)^2 - (1-s)^2 \left( \frac{1}{B_3} + \frac{3}{B_1} \right) \right)$ .

Here,  $f(\rho)$  and  $g(\rho)$  are the ratios of two polynomials in  $\rho$ . The non-negativity property of variance implies the expressions  $B_1\alpha_1 + \alpha_4\rho$ ,  $A_1\alpha_2 + \alpha_5\rho$ ,  $B_1^2\beta_1 + \beta_3\rho - \beta_5\rho^2$ , and  $A_1^2\beta_2 + \beta_4\rho - \beta_6\rho^2$  are non-negative. Additionally, the cases where these factors equal zero are independent of the discussion here. Thus, the denominators of  $f(\rho)$  and  $g(\rho)$  are positive, and therefore,  $f(\rho)$  and  $g(\rho)$  are partial differentiable functions with respect to  $\rho$ . Now the partial differential of  $f(\rho)$  with respect to  $\rho$ , denoted  $f'(\rho)$ , is given as

$$f'(\rho) = \frac{\alpha_3\rho(B_1\alpha_1(A_1\alpha_2 + \alpha_5\rho) + A_1\alpha_2(B_1\alpha_1 + \alpha_4\rho))}{((B_1\alpha_1 + \alpha_4\rho)(A_1\alpha_2 + \alpha_5\rho))^2}. \quad (\text{F14})$$

Since  $A_1$  and  $B_1$  are non-negative, it implies  $\alpha_1$  and  $\alpha_2$  are non-negative. Therefore, for  $\rho \geq 0$ ,  $f'(\rho)$  is non-negative, and hence  $f(\rho)$  is monotonically increase in  $\rho$ . Also the partial differential of  $g(\rho)$  with respect to  $\rho$ , denoted  $g'(\rho)$ , is given as:

$$g'(\rho) = \left\{ (1-q)(1-s)A_1B_1\beta_1^2\beta_2^2\rho[(B_1^2\beta_1 + \beta_5\rho^2)(A_1^2\beta_2 + \beta_4\rho - \beta_6\rho^2) + (B_1^2\beta_1 + \beta_3\rho - \beta_5\rho^2)(A_1^2\beta_2 + \beta_6\rho^2)] \right\} / \left\{ [(B_1^2\beta_1 + \beta_3\rho - \beta_5\rho^2)(A_1^2\beta_2 + \beta_4\rho - \beta_6\rho^2)]^2 \right\}. \quad (\text{F15})$$

If  $B_1^2\beta_1 + \beta_5\rho^2$  and  $A_1^2\beta_2 + \beta_6\rho^2$  are non-negative, then  $g'(\rho)$  is non-negative, and hence  $g(\rho)$  is monotonic increasing in  $\rho$ . Therefore, it suffices to show these two equations are non-negative. Now,

$$B_1^2\beta_1 + \beta_5\rho^2 \geq (1-s)^4\rho^2 \left( \frac{A_1}{2} \left( \frac{1}{1-q} + \frac{1-q}{A_2} \right) - \frac{(1-q)^3}{A_1} + \frac{1}{4}(1-q) \left( A \left( \frac{1}{1-q} + \frac{1-q}{A_2} \right)^2 - (1-q)^2 \left( \frac{1}{A_3} + \frac{3}{A} \right) \right) \right) = (1-s)^4\rho^2q(1-x)^3f(x, q),$$

where  $x = \cos \frac{2\pi}{m_1}$  and  $f(x, q) = 1 + 2(4 + 13x + 8x^2)q + 4(1 + 10x + 17x^2 - 8x^3 - 16x^4)q^2 + 2(4 + 15x + 8x^2 - 52x^3 - 144x^4 - 96x^5)q^3 + 2(3 - 52x^2 - 56x^3 + 184x^4 + 288x^5 + 96x^6)q^4 + 2(4 + 15x + 8x^2 - 52x^3 - 144x^4 - 96x^5)q^5 + 4(1 + 10x + 17x^2 - 8x^3 - 16x^4)q^6 + 2(4 + 13x + 8x^2)q^6 + q^8$ . Now, to show  $B_1^2\beta_1 + \beta_5\rho^2$  is non-negative, it suffices to show that the minimum value of  $f(x, q)$  is non-negative. To find the minimum value, we need to solve the system of equations:

$$\frac{\partial f(x, q)}{\partial q} = 0, \quad \frac{\partial f(x, q)}{\partial x} = 0.$$

The solutions to the above system of equations are mostly imaginary, but as  $x \in [-1, 1]$  and  $q \in [0, 1]$ , it has only two real solutions:  $\{x = -0.744169, q = 0.395297\}$  and  $\{x = -0.412305, y = 0\}$ <sup>1</sup>. The minimum value of  $f(x, q)$  would lie either at these critical points or the boundary of the region  $[-1, 1] \times [0, 1]$ .  $f(x, q)$  has a minimum value of 0 at the boundary points  $\{(1, 1), (-1, 1)\}$ . Similarly,  $A_1^2\beta_2 + \beta_6\rho^2$  is non-negative (interchanging  $q, m_1$  by  $s, m_2$  respectively, in  $B_1^2\beta_1 + \beta_5\rho^2$ ), and this implies  $g'(\rho)$  is non-negative when  $\rho \geq 0$ . Hence, if  $\rho \geq 0$ , then  $\rho_{1ss}^2$  and  $\rho_{1cc}^2$  are both monotonically increasing in  $\rho$ , which implies  $\rho_{1ss}^2 + \rho_{1cc}^2$  is monotonically increasing in  $\rho$ . For  $\rho < 0$ ,  $f'(\rho)$  (F14) and  $g'(\rho)$  (F15) are non-positive, and this implies  $\rho_{1ss}^2 + \rho_{1cc}^2$  is monotonic decreasing in  $\rho$ .

Now we consider  $\delta = -1$ . Let  $P_I(\cdot, \cdot)$  and  $P_{II}(\cdot, \cdot)$  denote the pmfs for the cases  $\delta = 1$  and  $\delta = -1$ , respectively. From the pmf given in (4), we obtain

$$\begin{aligned} P_{II} \left( \frac{2\pi k}{m_1}, \frac{2\pi(2\beta - l)}{m_2} \right) &= C_1 (q^{\zeta_1} + q^{m_1 - \zeta_1}) (s^{\zeta_2} + s^{m_2 - \zeta_2}) \left( 1 + \rho \cos \left( \frac{2\pi\zeta_1}{m_1} - \frac{2\pi\zeta_2}{m_2} \right) \right) \\ &= P_I \left( \frac{2\pi k}{m_1}, \frac{2\pi l}{m_2} \right), \quad \forall (k, l) \in \mathbf{Z}_{\mathbf{m}_1} \times \mathbf{Z}_{\mathbf{m}_2}. \end{aligned}$$

This establishes a one-to-one correspondence between the two cases. Thus, the result for the second case is a direct consequence of the first case.

## References

- [1] F. Ball and P. Blackwell. A finite form for the wrapped poisson distribution. *Advances in applied probability*, 24(1):221–222, 1992.
- [2] P. D. Clift and R. A. Plumb. *The Asian Monsoon: Causes, History and Effects*. Cambridge University Press, Cambridge, UK, 2008.

<sup>1</sup>Here, we solved the system of equations using Wolfram Mathematica

- [3] W. G. Cochran. Some Methods for Strengthening the Common  $X^2$  Tests. *Biometrics*, 10(4):417–451, 1954.
- [4] N. I. Fisher. *Statistical analysis of circular data*. cambridge university press, 1995.
- [5] F. Hassanzadeh and Z. Kalaylioglu. A new multimodal and asymmetric bivariate circular distribution. *Environmental and Ecological Statistics*, 25:363–385, 2018.
- [6] S. D. Horn. Goodness-of-fit tests for discrete data: A review and an application to a health impairment scale. *Biometrics*, 33(1):237–247, 1977.
- [7] S. Jacob and K. Jayakumar. Wrapped geometric distribution: A new probability model for circular data. *J. Stat. Theory Appl.*, 12(4):348–355, 2013.
- [8] S. R. Jammalamadaka and A. SenGupta. *Topics in Circular Statistics*, volume 5 of *Series on Multivariate Analysis*. WORLD SCIENTIFIC, 4 2001.
- [9] J. Jha and A. Biswas. Distribution and time-series modelling of ordinal circular data. *Environmetrics*, 29(2):e2490, 3 2018.
- [10] J. Jha and A. Biswas. Regression Models for Directional Variables. *Forum for Interdisciplinary Mathematics*, pages 333–348, 2022.
- [11] M. C. Jones, A. Pewsey, and S. Kato. On a class of circulas: copulas for circular distributions. *Annals of the Institute of Statistical Mathematics*, 67:843–862, 2015.
- [12] P. E. Jupp and K. V. Mardia. A general correlation coefficient for directional data and related regression problems. *Biometrika*, 67(1):163–173, 1980.
- [13] S. Kato and A. Pewsey. A möbius transformation-induced distribution on the torus. *Biometrika*, 102(2):359–370, 2015.
- [14] S. Kato, K. Shimizu, and G. S. Shieh. A circular–circular regression model. *Statistica Sinica*, 18(2):633–645, 2008.
- [15] F. Lagona. Regression analysis of correlated circular data based on the multivariate von mises distribution. *Environmental and ecological statistics*, 2016.
- [16] F. Lagona and M. Mingione. Copula-based models for correlated circular data. *arXiv preprint arXiv:2406.04085*, 2024.
- [17] K. V. Mardia. *Statistics of directional data*. Academic Press, 1972.
- [18] K. V. Mardia. Statistics of directional data. *Journal of the Royal Statistical Society Series B: Statistical Methodology*, 37(3):349–371, 1975.
- [19] K. V. Mardia and P. E. Jupp. *Directional statistics*. John Wiley & Sons, 2009.
- [20] K. V. Mardia, C. C. Taylor, and G. K. Subramaniam. Protein bioinformatics and mixtures of bivariate von mises distributions for angular data. *Biometrics*, 63(2):505–512, 2007.
- [21] A. SenGupta and B. C. Arnold, editors. *Directional Statistics for Innovative Applications*. Forum for Interdisciplinary Mathematics. Springer Nature Singapore, Singapore, 2022.
- [22] S. Singh. *Climatology*. Prayag Pustak Bhawan, Allahabad, n.d.
- [23] K. Takahashi and H. Arakawa, editors. *Climates of Southern and Western Asia*, volume 9 of *World Survey of Climatology*. Elsevier Scientific Publishing Company, Amsterdam and New York, 1981. Edited volume in the World Survey of Climatology series, Editor-in-Chief: H. E. Landsberg.

# S1 Supplement to “Some bivariate distributions on a discrete torus with application to wind direction datasets”

## S1.1 Remark 1

In the BWG distribution, the parameters  $\alpha$  and  $\beta$  are discrete, with  $\alpha \in \mathbf{Z}_{m_1}$  and  $\beta \in \mathbf{Z}_{m_2}$ . We generalize this model by allowing  $\alpha$  and  $\beta$  to vary continuously over the intervals  $[0, m_1)$  and  $[0, m_2)$ , respectively; we name this generalization the BGWG distribution. While Theorem 4 establishes the monotonicity of  $\rho_1^2$  for the BWG distribution, here we extend this result to the BGWG distribution. To simplify the derivation of  $\rho_1^2$ , without loss of generality, we assume the parameters  $\alpha$  and  $\beta$  lie within the interval  $(0, 1)$ . We use the following notation:

$$\begin{aligned} H_i &= \frac{1}{A_i} (1 - q^{m_1}) \left( q^\alpha - q^{2-\alpha} - q(q^\alpha - q^{-\alpha}) \cos \frac{2i\pi}{m_1} \right), \\ G_i &= \frac{1}{A_i} q (1 - q^{m_1}) (q^{-\alpha} - q^\alpha) \sin \frac{2i\pi}{m_1}, \\ N_i &= \frac{1}{B_i} (1 - s^{m_2}) \left( s^\beta - s^{2-\beta} - s(s^\beta - s^{-\beta}) \cos \frac{2i\pi}{m_2} \right), \\ M_i &= \frac{1}{B_i} s (1 - s^{m_2}) (s^{-\beta} - s^\beta) \sin \frac{2i\pi}{m_2}, \end{aligned}$$

where  $i \in \{0, 1, 2, 3\}$ .

The standard correlation formula is utilized to express the correlation coefficient  $\rho_1^2$ . The resulting general formula is given by

$$\rho_1^2 = \frac{\mathbf{h}_1(\mathbf{v})}{\mathbf{h}_2(\mathbf{v})}, \quad (\text{S1})$$

where

$$\begin{aligned} \mathbf{h}_1(\mathbf{v}) &= (\text{Cov}_{CC}^2 \text{Var}_{SX_2} + \text{Cov}_{CS}^2 \text{Var}_{CX_2}) \text{Var}_{SX_1} + (\text{Cov}_{SC}^2 \text{Var}_{SX_2} \\ &\quad + \text{Cov}_{SS}^2 \text{Var}_{CX_2}) \text{Var}_{CX_1} + 2(\text{Cov}_{CC} \text{Cov}_{SS} + \text{Cov}_{CS} \text{Cov}_{SC}) \\ &\quad \text{Cov}_1 \text{Cov}_2 - 2(\text{Cov}_{CC} \text{Cov}_{SC} \text{Var}_{SX_2} + \text{Cov}_{CS} \text{Cov}_{SS} \text{Var}_{CX_2}) \text{Cov}_1 \\ &\quad - 2(\text{Cov}_{CC} \text{Cov}_{SC} \text{Var}_{SX_1} + \text{Cov}_{SC} \text{Cov}_{SS} \text{Var}_{CX_1}) \text{Cov}_2, \end{aligned}$$

$$\mathbf{h}_2(\mathbf{v}) = (\text{Var}_{CX_1} \text{Var}_{SX_1} - \text{Cov}_1^2)(\text{Var}_{CX_2} \text{Var}_{SX_2} - \text{Cov}_2^2),$$

$\mathbf{v} = (q, \alpha, m_1, s, \beta, m_2, \rho)$ ,  $\text{Var}_{CX_j} = \text{var}(\cos X_j)$ ,  $\text{Var}_{SX_j} = \text{var}(\sin X_j)$ ,  $\text{Cov}_j = \text{cov}(\cos X_j, \sin X_j)$ ,  $\text{Cov}_{CC} = \text{cov}(\cos X_1, \cos X_2)$ ,  $\text{Cov}_{CS} = \text{cov}(\cos X_1, \sin X_2)$  etc., where  $j \in \{1, 2\}$ .

To verify the monotonicity of  $\rho_1^2$ , we examine two distinct cases.

**Case 1:**  $\delta = 1$

We compute the required covariance and variance terms using the following moments given below:

$$\begin{aligned} \text{E}_{CX_1} &= C_7 \left[ H_1 N_0 + \frac{1}{2} \rho [(H_2 N_1 + G_2 M_1 + H_0 N_1) \cos \phi - (H_2 M_1 - G_2 N_1 + H_0 M_1) \sin \phi] \right], \\ \text{E}_{CX_2} &= C_7 \left[ H_0 N_1 + \frac{1}{2} \rho [(H_1 N_0 + H_1 N_2 + G_1 M_2) \cos \phi + (G_1 N_0 - H_1 M_2 + G_1 N_2) \sin \phi] \right], \end{aligned}$$

$$\begin{aligned}
E_{SX_1} &= C_7 \left[ G_1 N_0 + \frac{1}{2} \rho \left[ (H_0 M_1 - H_2 M_1 + G_2 N_1) \cos \phi + (H_0 N_1 - H_2 N_1 - G_2 M_1) \sin \phi \right] \right], \\
E_{SX_2} &= C_7 \left[ H_0 M_1 + \frac{1}{2} \rho \left[ (G_1 N_0 + H_1 M_2 - G_1 N_2) \cos \phi + (H_1 N_2 + G_1 M_2 - H_1 N_0) \sin \phi \right] \right], \\
E_{CCX_1} &= \frac{1}{2} C_7 \left[ H_0 N_0 + H_2 N_0 + \frac{1}{2} \rho \left[ [(3H_1 + H_3)N_1 + (G_1 + G_3)M_1] \cos \phi - [(3H_1 + H_3)M_1 \right. \right. \\
&\quad \left. \left. - (G_1 + G_3)N_1] \sin \phi \right] \right], \\
E_{CCX_2} &= \frac{1}{2} C_7 \left[ H_0 N_0 + H_0 N_2 + \frac{1}{2} \rho \left[ [(3N_1 + N_3)H_1 + (M_1 + M_3)G_1] \cos \phi - [(M_1 + M_3)H_1 \right. \right. \\
&\quad \left. \left. - (3N_1 + N_3)G_1] \sin \phi \right] \right], \\
E_{SSX_1} &= \frac{1}{2} C_7 \left[ H_0 N_0 - H_2 N_0 + \frac{1}{2} \rho \left[ [(H_1 - H_3)N_1 + (3G_1 - G_3)M_1] \cos \phi - [(H_1 - H_3)M_1 \right. \right. \\
&\quad \left. \left. - (3G_1 - G_3)N_1] \sin \phi \right] \right], \\
E_{SSX_2} &= \frac{1}{2} C_7 \left[ H_0 N_0 - H_0 N_2 + \frac{1}{2} \rho \left[ [(N_1 - N_3)H_1 + (3M_1 - M_3)G_1] \cos \phi - [(3M_1 - M_3)H_1 \right. \right. \\
&\quad \left. \left. - (N_1 - N_3)G_1] \sin \phi \right] \right], \\
E_{CC} &= C_7 \left[ H_1 N_1 + \frac{1}{4} \rho \left[ (H_2 N_0 + H_0 N_2 + H_2 N_2 + G_2 M_2 + H_0 N_0) \cos \phi + (G_2 N_0 - H_0 M_2 \right. \right. \\
&\quad \left. \left. - H_2 M_2 + G_2 N_2) \sin \phi \right] \right], \\
E_{CS} &= C_7 \left[ H_1 M_1 + \frac{1}{4} \rho \left[ (G_2 N_0 + H_0 M_2 - G_2 N_2 + H_2 M_2) \cos \phi + (H_0 N_2 - H_2 N_0 + H_2 N_2 \right. \right. \\
&\quad \left. \left. + G_2 M_2 - H_0 N_0) \sin \phi \right] \right], \\
E_{SC} &= C_7 \left[ G_1 N_1 + \frac{1}{4} \rho \left[ (G_2 N_0 + H_0 M_2 - H_2 M_2 + G_2 N_2) \cos \phi + (H_0 N_2 - H_2 N_0 - H_2 N_2 \right. \right. \\
&\quad \left. \left. - G_2 M_2 + H_0 N_0) \sin \phi \right] \right], \\
E_{SS} &= C_7 \left[ G_1 M_1 - \frac{1}{4} \rho \left[ (H_2 N_0 + H_0 N_2 - H_2 N_2 - G_2 M_2 - H_0 N_0) \cos \phi + (G_2 N_0 - H_0 M_2 \right. \right. \\
&\quad \left. \left. + H_2 M_2 - G_2 N_2) \sin \phi \right] \right], \\
E_{X_1} &= \frac{1}{2} C_7 \left[ G_2 N_0 + \frac{1}{2} \rho \left[ (H_1 M_1 - H_3 M_1 + G_1 N_1 + G_3 N_1) \cos \phi + (H_1 N_1 - H_3 N_1 - G_1 M_1 \right. \right. \\
&\quad \left. \left. - G_3 M_1) \sin \phi \right] \right], \\
E_{X_2} &= \frac{1}{2} C_7 \left[ H_0 M_2 + \frac{1}{2} \rho \left[ (M_1 H_1 + M_3 H_1 + N_1 G_1 - N_3 G_1) \cos \phi + (N_3 H_1 - N_1 H_1 + M_1 G_1 \right. \right. \\
&\quad \left. \left. + M_3 G_1) \sin \phi \right] \right],
\end{aligned}$$

where  $\phi = \left( \frac{2\pi\alpha}{m_1} - \frac{2\pi\beta}{m_2} \right)$ ,  $E_{CC} = E(\cos X_1 \cos X_2)$ ,  $E_{CS} = E(\cos X_1 \sin X_2)$ ,  $E_{CX_i} = E(\cos X_i)$ ,  $E_{CCX_i} = E(\cos^2 X_i)$ ,  $E_{X_i} = E(\cos X_i \sin X_i)$ , etc.,  $i \in \{1, 2\}$  and  $E(\cdot)$  denotes the expectation.

To verify the monotonicity of  $\rho_1^2$ , we first demonstrate that it is partially differentiable with respect to  $\rho$ . Next, we identify the regions where the partial derivative is positive or negative.

The coefficients  $\rho'_1$  and  $\rho'_2$  denote the correlations between  $\cos X_1$  and  $\sin X_1$ , and  $\cos X_2$  and  $\sin X_2$ , respectively. These two pairs are not perfectly correlated except for the case  $m_1, m_2 \in \mathbf{Z}_3 \setminus \{0\}$ . This is because for any given  $k_1$  and  $k_2$ , the equation  $\cos Y = k_1 \sin Y + k_2$  has at most two solutions in the range  $[0, 2\pi]$ . However, no such pair  $(k_1, k_2)$  exists except for the degenerate BGWG distribution. Consequently,  $(1 - \rho'^2_1)(1 - \rho'^2_2) > 0$ , and this inequality implies  $h_2(\mathbf{v}) > 0$ . Thus,  $\rho^2_1$  can be expressed as the ratio of two polynomials in  $\rho$ , and the polynomial corresponding to  $h_2(\mathbf{v})$  has no roots within the parameter space. Therefore, it is partially differentiable with respect to  $\rho$ , and its derivative is given as,

$$\frac{\partial \rho^2_1}{\partial \rho} = \frac{\tau(\mathbf{v})}{h_2(\mathbf{v})^2}, \quad (\text{S2})$$

where  $\tau(\mathbf{v}) = h'_1(\mathbf{v})_\rho h_2(\mathbf{v}) - h_1(\mathbf{v}) h'_2(\mathbf{v})_\rho$ , and  $h'_1(\mathbf{v})_\rho$  and  $h'_2(\mathbf{v})_\rho$  represent the partial derivative of  $h_1(\mathbf{v})$  and  $h_2(\mathbf{v})$  with respect to  $\rho$ , respectively. Now, instead of checking whether  $\frac{\partial \rho^2_1}{\partial \rho}$  is positive or not, it is more convenient to check  $\tau(\mathbf{v})$  as  $h_2(\mathbf{v})^2$  is always positive. So the function  $\tau(\cdot)$  is optimized in the regions  $\otimes_1 = \left\{ \{q, s\} \in [0, 1], \{\alpha, \beta\} \in [0, 1], \{m_1, m_2\} \in \mathbf{K}_n, \rho \in [-1, 0] \right\}$  and  $\otimes_2 = \left\{ \{q, s\} \in [0, 1], \{\alpha, \beta\} \in [0, 1], \{m_1, m_2\} \in \mathbf{K}_n, \rho \in [0, 1] \right\}$ , where  $\mathbf{K}_n = \{1, 2, \dots, n\}$  and  $n$  is the natural number. To handle the challenge of optimizing in the mixed (continuous and discrete) regions  $\otimes_1$  and  $\otimes_2$  mentioned above, we assume  $m_1, m_2 \in [1, n]$ . The optimization process is done in ‘Wolfram-Mathematica’ using ‘NMinimize’ and ‘NMaximize’ functions with the ‘Nelder-Mead’ method and utilizes the ‘Round’ function for the integer values of  $m_1$  and  $m_2$ .

**Table S1:** Optimal Values of  $\tau(\mathbf{v})$

Region	Minimum Value of $\tau(\mathbf{v})$	Maximum Value of $\tau(\mathbf{v})$
$\otimes_1, n = 100$	-0.004 (0.999, 0.018, 086, 0.999, 0.382, 099, -1.000)	0 (0.269, 0.910, 0098, 0.005, 0.229, 085, -0.546)
$\otimes_2, n = 100$	0 (0.009, 0.800, 100, 0.046, 0.892, 098, 0.077)	0.004 (0.999, 0.000, 004, 0.999, 0.128, 100, 1.000)
$\otimes_1, n = 300$	-0.004 (0.998, 0.0419, 003, 0.999, 0.998, 258, -1.000)	0 (0.000, 0.951, 193, 0.116, 0.372, 181, -0.331)
$\otimes_2, n = 300$	0 (0.002, 0.769, 300, 0.009, 0.904, 300, 0.047)	0.004 (0.998, 0.659, 005, 0.999, 0.003, 149, 1.000)
$\otimes_1, n = 600$	-0.004 (0.999, 0.999, 016, 0.999, 0.521, 195, -1.000)	0 (0.003, 0.991, 180, 0.063, 0.338, 530, -0.004)
$\otimes_2, n = 600$	0 (0.064, 0.744, 488, 0.035, 0.963, 553, 0.081)	0.004 (0.999, 0.603, 016, 0.999, 0.481, 187, 1.000)

**Table S1** shows the optimal values of  $\tau(\cdot)$ , evaluated in the regions  $\otimes_1$  and  $\otimes_2$ , with distinct values of  $n$ . From the table, it is clear that the function  $\tau(\cdot)$  attains the maximum

value in the region  $\otimes_1$ , which is a non-positive number, and the minimum value in the region  $\otimes_2$ , which is a non-negative number. Therefore, the  $\rho_1^2$  is monotonically decreasing in the region  $\otimes_1$  and monotonically increasing in the region  $\otimes_2$  with respect to  $\rho$ .

**Case 2:**  $\delta = -1$  In this Case, to compute  $\rho_1^2$  we use the following moments

$$\begin{aligned}
E_{CX_1} &= C_7 \left[ H_1 N_0 + \frac{\rho}{2} \left[ (H_2 N_1 - G_2 M_1 + H_0 N_1) \cos \psi + (H_2 M_1 + G_2 N_1 + H_0 M_1) \sin \psi \right] \right], \\
E_{CX_2} &= C_7 \left[ H_0 N_1 + \frac{\rho}{2} \left[ (H_1 N_2 - G_1 M_2 + H_1 N_0) \cos \psi + (H_1 M_2 + G_1 N_2 + G_1 N_0) \sin \psi \right] \right], \\
E_{SX_1} &= C_7 \left[ G_1 N_0 + \frac{\rho}{2} \left[ (H_2 M_1 + G_2 N_1 - H_0 M_1) \cos \psi + (G_2 M_1 - H_2 N_1 + H_0 N_1) \sin \psi \right] \right], \\
E_{SX_2} &= C_7 \left[ H_0 M_1 + \frac{\rho}{2} \left[ (H_1 M_2 + G_1 N_2 - G_1 N_0) \cos \psi + (G_1 M_2 - H_1 N_2 + H_1 N_0) \sin \psi \right] \right], \\
E_{CCX_1} &= \frac{C_7}{2} \left[ H_0 N_0 + H_2 N_0 + \frac{\rho}{2} \left[ (3H_1 N_1 - G_1 M_1 + H_3 N_1 - G_3 M_1) \cos \psi + (3H_1 M_1 + G_1 N_1 \right. \right. \\
&\quad \left. \left. + H_3 M_1 + G_3 N_1) \sin \psi \right] \right], \\
E_{CCX_2} &= \frac{C_7}{2} \left[ H_0 N_0 + H_0 N_2 + \frac{\rho}{2} \left[ (3H_1 N_1 - G_1 M_1 + H_1 N_3 - G_1 M_3) \cos \psi + (H_1 M_1 + 3G_1 N_1 \right. \right. \\
&\quad \left. \left. + H_1 M_3 + G_1 N_3) \sin \psi \right] \right], \\
E_{SSX_1} &= \frac{C_7}{2} \left[ H_0 N_0 - H_2 N_0 + \frac{\rho}{2} \left[ (H_1 N_1 - 3G_1 M_1 - H_3 N_1 + G_3 M_1) \cos \psi + (H_1 M_1 + 3G_1 N_1 \right. \right. \\
&\quad \left. \left. - H_3 M_1 - G_3 N_1) \sin \psi \right] \right], \\
E_{SSX_2} &= \frac{C_7}{2} \left[ H_0 N_0 - H_0 N_2 + \frac{\rho}{2} \left[ (H_1 N_1 - 3G_1 M_1 - H_1 N_3 + G_1 M_3) \cos \psi + (3H_1 M_1 + G_1 N_1 \right. \right. \\
&\quad \left. \left. - H_1 M_3 - G_1 N_3) \sin \psi \right] \right], \\
E_{CC} &= C_7 \left[ H_1 N_1 + \frac{\rho}{4} \left[ (H_2 N_2 - G_2 M_2 + H_0 N_0 + H_2 N_0 + H_0 N_2) \cos \psi + (H_2 M_2 + G_2 N_2 \right. \right. \\
&\quad \left. \left. + G_2 N_0 + H_0 M_2) \sin \psi \right] \right], \\
E_{CS} &= C_7 \left[ H_1 M_1 + \frac{\rho}{4} \left[ (H_2 M_2 + G_2 N_2 - G_2 N_0 + H_0 M_2) \cos \psi + (G_2 M_2 - H_2 N_2 + H_0 N_0 \right. \right. \\
&\quad \left. \left. + H_2 N_0 - H_0 N_2) \sin \psi \right] \right], \\
E_{SC} &= C_7 \left[ G_1 N_1 + \frac{\rho}{4} \left[ (H_2 M_2 + G_2 N_2 + G_2 N_0 - H_0 M_2) \cos \psi - (H_2 N_2 - G_2 M_2 - H_0 N_0 \right. \right. \\
&\quad \left. \left. + H_2 N_0 - H_0 N_2) \sin \psi \right] \right], \\
E_{SS} &= C_7 \left[ G_1 M_1 - \frac{\rho}{4} \left[ (H_2 N_2 - G_2 M_2 + H_0 N_0 - H_2 N_0 - H_0 N_2) \cos \psi + (H_2 M_2 + G_2 N_2 \right. \right. \\
&\quad \left. \left. - G_2 N_0 - H_0 M_2) \sin \psi \right] \right], \\
E_{X_1} &= \frac{C_7}{2} \left[ G_2 N_0 + \frac{\rho}{2} \left[ (H_3 M_1 + G_3 N_1 - H_1 M_1 + G_1 N_1) \cos \psi + (H_1 N_1 + G_1 M_1 - H_3 N_1 \right. \right. \\
&\quad \left. \left. + G_3 M_1) \sin \psi \right] \right], \\
E_{X_2} &= \frac{C_7}{2} \left[ H_0 M_2 + \frac{\rho}{2} \left[ (H_1 M_1 + H_1 M_3 - G_1 N_1 + G_1 N_3) \cos \psi + (H_1 N_1 - H_1 N_3 + G_1 M_1 \right. \right. \\
&\quad \left. \left. + G_1 M_3) \sin \psi \right] \right],
\end{aligned}$$

where  $\psi = \left( \frac{2\pi\alpha}{m_1} + \frac{2\pi\beta}{m_2} \right)$ .

We have already verified that  $\rho_1^2$  in (S1) is partially differentiable with respect to  $\rho$  in Case I. The differentiability in Case II follows directly from the same arguments. To verify the monotonicity of  $\rho_1^2$ , we analyze the extrema of  $\tau(\mathbf{v})$ . The optimal values of  $\tau(\cdot)$  are presented in [Table S2](#).

**Table S2:** Optimal Values of  $\tau(\mathbf{v})$

Region	Minimum Value of $\tau(\mathbf{v})$	Maximum Value of $\tau(\mathbf{v})$
$\otimes_1, n = 100$	-0.004 (0.999, 0.030, 0.999, 0.999, 0.074, 0.094, -1.000)	0 (0.269, 0.909, 0.098, 0.005, 0.229, 0.085, 0.546)
$\otimes_2, n = 100$	0 (0.009, 0.800, 100, 0.046, 0.892, 0.098, 0.077)	0.004 (0.999, 0.129, 100, 0.999, 0.086, 1.000)
$\otimes_1, n = 300$	-0.004 (0.999, 0.257, 009, 0.999, 0.535, 109, -1.000)	0 (0.000, 0.951, 193, 0.116, 0.372, 181, -0.331)
$\otimes_2, n = 300$	0 (0.002, 0.769, 300, 0.009, 0.904, 300, 0.047)	0.004 (0.999, 0.199, 003, 0.999, 0.538, 103, 1.000)
$\otimes_1, n = 600$	-0.004 (0.999, 0.999, 017, 0.999, 0.481, 196, -1.000)	0 (0.000, 0.951, 385, 0.116, 0.372, 562, -0.331)
$\otimes_2, n = 600$	0 (0.064, 0.744, 488, 0.035, 0.962, 553, 0.081)	0.004 (0.999, 0.557, 017, 0.999, 0.477, 188, 1.000)

[Table S2](#) shows the optimal values of  $\tau(\cdot)$ , evaluated in the regions  $\otimes_1 \times \otimes_2$ , with distinct values of  $n$ . From the table, it is clear that the function  $\tau(\cdot)$  attains the maximum value in the region  $\otimes_1$ , which is a non-positive number, and the minimum value in the region  $\otimes_2$ , which is a non-negative number. Therefore, the  $\rho_1^2$  is monotonically decreasing in the region  $\otimes_1$  and monotonically increasing in the region  $\otimes_2$  with respect to  $\rho$ .

## S1.2 Dataset-I

We perform a goodness-of-fit test using Pearson's chi-square test, where  $H_0$  and  $H_a$  denote the null and alternative hypotheses, respectively:

- $H_0$  : *Dataset-I* is a random sample from a BGWG distribution.
- $H_a$  : *Dataset-I* is not a random sample from a BGWG distribution.

To compute the chi-square test statistic ( $X^2$ ), we convert the expected frequency table into an array in such a way that the first row is left to right, followed by the second row in the same order, and so on. Therefore, this process results in 256 cells; however, most of these cells have an expected frequency that is very small. According to [3] and [6], "the expected frequency of each cell should be  $> 1$ , and at least 80% of them should be  $\geq 5$ ." Therefore, we merge the cells into 16 groups in accordance with this requirement, and [Table S3](#) represents the groups with respective frequencies.

**Table S3:** Groups with expected and observed frequencies

Groups	1:13 126:150	14:17 151:175	18:31 176:192	32:45 193:207	46:60 208:212	61:77 213:225	78:100 226:240	101:125 241:256
E. freq.	5.835 5.134	5.197 5.178	5.725 5.117	5.105 5.268	5.279 4.370	5.312 5.464	5.189 7.972	5.277 11.577
O. freq.	6 3	3 4	3 2	7 2	8 5	8 7	9 11	5 10

The test statistic  $X^2$  comes out 15.479, and the Chi-square  $\chi^2$  value with 9 degrees of freedom at the significance level of 0.05 is 16.919, which is greater than the  $X^2$  value. Thus, we fail to reject the null hypothesis  $H_0$  at this significance level.

### S1.2.1 Analysis using the BWG Distribution

We estimate the parameters of BWG distribution, and [Table S4](#) represents the estimated parameters.

**Table S4:** Estimated parameters of BWG for *Dataset-I*

Parameters	Estimates (Sd Error)
$\hat{q}_{MLE}$	0.817 (0.040)
$\hat{s}_{MLE}$	0.801 (0.040)
$\hat{\rho}_{MLE}$	0.815 (0.118)
$\hat{\alpha}_{MLE}$	15
$\hat{\beta}_{MLE}$	15
$\hat{\delta}_{MLE}$	-1
AIC	978.786

**Interpretation:** The estimates  $\hat{\rho}_{MLE} = 0.815$  and  $\hat{\delta}_{MLE} = -1$  indicate an anti-rotational dependency.

## S1.3 Dataset-II

We perform the goodness-of-fit test for BGWG such that,

- $H_0$  : *Dataset-II* is a random sample from BGWG distribution.
- $H_a$  : *Dataset-II* is not a random sample from BGWG distribution.

There are 256 cells, and the expected frequency of most of the cells is very small; therefore, we merge the cells into 15 groups, and [Table S5](#) represents these groups with their respective frequencies.

The test statistic  $X^2$  comes out to 14.807, and the  $\chi^2$  value with 8 degrees of freedom at the significance level of 0.05 is 15.507, which is greater than the  $X^2$  value. Thus, we fail to reject the null hypothesis  $H_0$  at this significance level.

**Table S5:** Groups with expected and observed frequencies

Groups	1:6 33:34	7:17 35:38	18:19 39:43	20:21 44:46	22:23 47:48	24:27 49:64	28:30 65:256	31:32
E. freq.	7.996 6.231	5.231 6.811	5.659 6.029	9.668 6.578	6.932 8.175	5.845 9.587	6.465 9.145	5.649
O. freq.	13 7	6 7	3 5	3 9	6 11	3 9	6 9	9

### S1.3.1 Analysis using the BWG Distribution

We estimate the parameters of BWG distribution, and [Table S6](#) represents the estimates of the parameters.

**Table S6:** Estimated parameters of BWG for *Dataset-II*

Parameters	Estimates (Sd. Error)
$\hat{q}_{MLE}$	0.295 (0.030)
$\hat{s}_{MLE}$	0.567 (0.035)
$\hat{\rho}_{MLE}$	-0.928 (0.046)
$\hat{\alpha}_{MLE}$	1
$\hat{\beta}_{MLE}$	1
$\hat{\delta}_{MLE}$	1
AIC	919.6717

**Interpretation:** The estimate  $\hat{\rho}_{MLE} = -0.928$  indicates a strong dependency between the wind directions of Marina Beach, Chennai and Gwalior Fort.

## S1.4 Dataset-III

We perform the goodness-of-fit test for BGWG such that,

- $H_0$  : *Dataset-III* is a random sample from BGWG distribution.
- $H_a$  : *Dataset-III* is not a random sample from BGWG distribution.

There are 256 cells, and the expected frequency of most of the cells is very small; therefore, we merge the cells into 15 groups, and [Table S7](#) represents these groups with their respective frequencies.

The test statistic  $X^2$  comes out 10.023, and the Chi-square  $\chi^2$  value with 8 degrees of freedom at the significance level of 0.05 is 15.507, which is greater than the  $X^2$  value. Thus, we fail to reject the null hypothesis  $H_0$  at this significance level.

### S1.4.1 Analysis using the BWG Distribution

We estimate the parameters of BWG distribution, and [Table S8](#) represents the estimates of the parameters.

**Table S7:** Groups with expected and observed frequencies

Groups	1:14	15:17	18:20	21:27	28:30	31:32	33:34	35:36
	37:38	39:45	46:47	48:50	51:57	58:75	76:256	
E. freq.	7.353 5.001	6.151 6.569	9.830 5.751	6.526 5.990	7.081 5.178	7.524 5.019	8.412 5.052	7.563
O. freq.	10 4	6 10	9 9	8 5	4 5	4 4	6 7	8

**Table S8:** Estimated parameters of BWG for *Dataset-III*

Parameters	Estimates (Sd. Error)
$\hat{q}_{MLE}$	0.370 (0.035)
$\hat{s}_{MLE}$	0.999 (0.001)
$\hat{\rho}_{MLE}$	-0.830 (0.102)
$\hat{\alpha}_{MLE}$	2
$\hat{\beta}_{MLE}$	9
$\hat{\delta}_{MLE}$	1
AIC	851.388

**Interpretation:** The estimate  $\hat{\rho}_{MLE} = -0.830$  indicates a strong dependency between the wind directions of Marina Beach, Chennai and Rao Circle, Mangaluru.